2023

Geometric and Combinatorial Properties of Lattice Polytopes Defined from Graphs

Kaitlin Bruegge

University of Kentucky, kebr266@uky.edu

Author ORCID Identifier:

iD https://orcid.org/0000-0002-9083-6834

Digital Object Identifier: https://doi.org/10.13023/etd.2023.297

Right click to open a feedback form in a new tab to let us know how this document benefits you.

STUDENT AGREEMENT:

I represent that my thesis or dissertation and abstract are my original work. Proper attribution has been given to all outside sources. I understand that I am solely responsible for obtaining any needed copyright permissions. I have obtained needed written permission statement(s) from the owner(s) of each third-party copyrighted matter to be included in my work, allowing electronic distribution (if such use is not permitted by the fair use doctrine) which will be submitted to UKnowledge as Additional File.

I hereby grant to The University of Kentucky and its agents the irrevocable, non-exclusive, and royalty-free license to archive and make accessible my work in whole or in part in all forms of media, now or hereafter known. I agree that the document mentioned above may be made available immediately for worldwide access unless an embargo applies.

I retain all other ownership rights to the copyright of my work. I also retain the right to use in future works (such as articles or books) all or part of my work. I understand that I am free to register the copyright to my work.

REVIEW, APPROVAL AND ACCEPTANCE

The document mentioned above has been reviewed and accepted by the student's advisor, on behalf of the advisory committee, and by the Director of Graduate Studies (DGS), on behalf of the program; we verify that this is the final, approved version of the student's thesis including all changes required by the advisory committee. The undersigned agree to abide by the statements above.

<div align="right">

Kaitlin Bruegge, Student

Dr. Benjamin Braun, Major Professor

Dr. Benjamin Braun, Director of Graduate Studies

</div>

Geometric and Combinatorial Properties of Lattice Polytopes Defined from Graphs

---
DISSERTATION

A dissertation submitted in partial
fulfillment of the requirements for
the degree of Doctor of Philosophy
in the College of Arts and Sciences
at the University of Kentucky

By
Kaitlin Elizabeth Bruegge
Lexington, Kentucky

Director: Dr. Benjamin Braun, Professor of Mathematics
Lexington, Kentucky
2023

https://orcid.org/0000-0002-9083-6834

ABSTRACT OF DISSERTATION

Geometric and Combinatorial Properties of Lattice Polytopes Defined from Graphs

Polytopes are geometric objects that generalize polygons in the plane and polyhedra in 3-dimensional space. Of particular interest in geometric combinatorics are families of lattice polytopes defined from combinatorial objects, such as graphs. In particular, this dissertation studies symmetric edge polytopes (SEPs), defined from simple undirected graphs. In 2019, Higashitani, Jochemko, and Michałek gave a combinatorial description of the hyperplanes that support facets of a symmetric edge polytope in terms of certain labelings of the underlying graph.

Using this framework, we explore the number of facets that can be attained by the symmetric edge polytopes for graphs with certain structure. First, we establish formulas or bounds for the number of facets attained by families of sparse, connected graphs, and give conjectures concerning the maximum and minimum facet counts for more general families. We also consider the number of facets of SEPs arising from graphs generated by several random graph models and investigate a conjectured connection between facet counts for SEPs and clustering metrics on their underlying graphs.

KEYWORDS: lattice polytope, symmetric edge polytope, facet, random graph

Kaitlin Elizabeth Bruegge

June 14, 2023

Geometric and Combinatorial Properties of Lattice Polytopes Defined from Graphs

By
Kaitlin Elizabeth Bruegge

_____
Dr. Benjamin Braun
Director of Dissertation

_____
Dr. Benjamin Braun
Director of Graduate Studies

_____
June 14, 2023
Date

To family, friends, supporters, and residents of POT 702,
I couldn't have done it without you.

ACKNOWLEDGMENTS

I have been honored to receive an overwhelming amount of support, encouragement, and inspiration from so many incredible people over the past five years and long before. There are not words enough to thank them all sufficiently, but that certainly won't stop me from trying.

Graduate school has been the most frustrating and rewarding experience of my life so far. I have grown so much as a researcher, teacher, and friend, and none of it would have been possible without the amazing people I've met during this time. Even before he was my advisor, Dr. Ben Braun was an invaluable lifeline in figuring out who I am as a mathematician. I will forever be grateful for the genuine care and thoughtfulness that shines through every conversation we have about math and about life. All of my collaborators and coauthors in research have pushed me toward a deeper and broader understanding of mathematics. Thank you to Ben, Martha, Khrystyna, Matias, Derek, Zach, Jonah, Ford, Williem, Chloé, Rob, Ayah, Sasha, Uwe, Martina, and Matt for exploring some beautiful math with me. I will always cherish the friendships I've made in graduate school. In particular, I am so thankful to Angela, Courtney, and Lewis for the countless vent sessions, sanity checks, and silly little treats. I regret to inform you that you are now stuck with me forever, sorry about your luck. To all of these people, and many other friends and mentors, I am so grateful to know you.

My family did not always understand why I decided to do the whole PhD thing. Nevertheless, their unwavering support carried me through the days when even I didn't understand why I was doing the whole PhD thing. First, foremost, and always, I owe everything to my parents. Jim and Barb Bruegge never once let me believe

there was something I couldn't do. They, along with aunts, uncles, and cousins too numerous to name, have loved me through every moment of my 27 years and reminded me to be grateful for every crazy opportunity. Finally, I am incredibly lucky to have many friends whom I also count as family. Jenny, Maria, Mikaila, Ashley, and Laura, you have been there through pretty much everything. You are my sisters, and there is nothing you can do about it!

To all of these people and the many more I could name given infinite space and time, thank you. You've made this seemingly impossible thing feel only improbable.

TABLE OF CONTENTS

LIST OF TABLES

Chapter 1 Introduction and Background

1.1   Introduction

This dissertation contains results, conjectures, and questions related to two projects, each of which is focused on the study of symmetric edge polytopes, a family of lattice polytopes defined from simple, undirected graphs. Chapter 1 gives necessary background information concerning lattice polytopes, including some popular areas of study and the introduction of our structure of interest, the symmetric edge polytope. This chapter also sets the scene for where the work of this dissertation fits in the community more broadly. The results in Chapters 2 and 3 make progress toward the goal of understanding how the structure of a graph impacts the number of facets of its symmetric edge polytope. Chapter 2 focuses on determining bounds for the number of facets attainable by a symmetric edge polytope for a graph with a fixed number of vertices. Chapter 3 explores what can be said about the symmetric edge polytopes for graphs generated by three different random graph models. Finally, Chapter 4 gives a further description of some of the computational techniques used and experiments conducted throughout this work.

1.2   Lattice Polytopes

1.2.1   Essential Definitions

Polytopes are geometric objects that generalize the notion of a polygon in the plane or a polyhedron in 3-dimensional space to real spaces of any dimension ($\mathbb{R}^n$). Figure 1.1 presents some examples of polytopes in $\mathbb{R}^3$ that may be familiar.
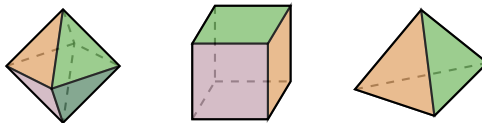
Figure 1.1:   The *octahedron*, *cube*, and *tetrahedron* above are examples of 3-dimensional polytopes, or *polyhedra*, obtained by taking the convex hull of points in $\mathbb{R}^3$. The tetrahedron is also a 3-simplex.

The study of polytopes is an active area of inquiry in geometric combinatorics and has a variety of applications. For example, polytopes naturally arise as the feasible regions in linear programming problems. When defined using other algebraic or combinatorial objects (e.g. permutations, matroids, graphs), the structure of the polytope can give interesting insights into their defining objects, and vice versa.

For any positive integer n, a polytope contained in $\mathbb{R}^n$ is a convex subset of points that can be defined in two ways, each derived from an attribute of its boundary. The first describes a polytope as a *convex hull* of points.

Definition 1.2.1. For a set of points $X \subseteq \mathbb{R}^d$, the *convex hull*, $\text{conv}\{X\}$, is the intersection of all convex sets containing X.

For finite sets,

$$\text{conv}\{v_1, v_2, \ldots, v_n\} = \left\{ \sum_{i=1}^{n} \lambda_i v_i \; : \; \lambda_i \geq 0, \; \sum \lambda_i = 1 \right\}.$$

When the set X is finite and irredundant, meaning that no point in X lies in the convex hull of the others, the points in X are called the *vertices* of $\text{conv}\{X\}$. These vertices span an *affine subspace* of $\mathbb{R}^n$, which we can visualize as some linear subspace that has been shifted away from the origin.

Definition 1.2.2. Given a d-dimenisonal vector space $L \subseteq \mathbb{R}^n$, a d-dimensional *affine subspace parallel to L* is of the form $v_0 + L$ for some $v_0 \in \mathbb{R}^n$.

On the other hand, given points (or vectors) $v_0, v_1, \ldots, v_m \in \mathbb{R}^n$, the *affine span* of these $m + 1$ points is given by

$$\left\{ \sum_{i=0}^{m} \alpha_i v_i \; : \; \alpha_i \in \mathbb{R}, \; \sum \alpha_i = 1 \right\}.$$

The *dimension* of a polytope is the dimension of the affine space spanned by its vertices. Putting this all together gives the following description of a polytope, called the $\mathcal{V}$-*description*.

Definition 1.2.3. A subset $P \subset \mathbb{R}^n$ is a *d-dimensional (convex) polytope* if

$$P = \text{conv}\{\mathbf{v}_1, \ldots, \mathbf{v}_m\}$$

such that the vertices $\mathbf{v}_1, \ldots, \mathbf{v}_m \in \mathbb{R}^n$ span a d-dimensional affine subspace of $\mathbb{R}^n$. Additionally, if the vertices lie in the *integer lattice* $\mathbb{Z}^n$, we say that P is a d-dimensional *lattice polytope*.

Example 1.2.4. The polytope P in Figure 1.2 is a cube in $\mathbb{R}^2$ obtained as the product of two copies of the interval $[-1, 1] \subset \mathbb{R}$. We can describe P by its vertices as

$$P := \text{conv}\{(-1, -1), \, (1, -1), \, (-1, 1), \, (1, 1)\}.$$

If a collection of $d + 1$ points span an d-dimensional affine subspace of $\mathbb{R}^d$ (i.e. the points are *affinely independent*), the convex hull of those points is called a *d-simplex*. For example, the tetrahedron in Figure 1.1 is a 3-simplex. Further, the simplex in $\mathbb{R}^d$ defined as the convex hull of the origin and the standard basis vectors $e_1, \ldots e_d$ is called the *standard d-simplex*, denoted by Δ_d.

The second definition describes a d-dimensional polytope as the intersection of closed halfspaces, each of which is bounded by a $(d - 1)$-dimensional hyperplane.

Definition 1.2.5. A hyperplane H is a *support hyperplane* of the polytope P if P is contained in one of the two closed halfspaces bounded by H and the intersection $H \cap P$ is nonempty.

The intersection $F = H \cap P$ is called a *face* of P. For a d-dimensional polytope, any face of dimension $d - 1$ is called a *facet*.
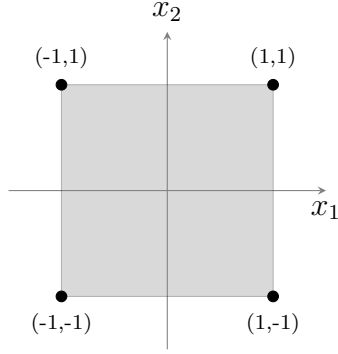
Figure 1.2: A 2-dimensional cube, $[-1,1]^2$.

Every polytope has a unique irredundant description as an intersection of halfspaces, called the $\mathcal{H}$-*description*. Since every support hyperplane can be encoded as a linear equation, the $\mathcal{H}$-description can be written as a system of linear inequalities. Each inequality in the $\mathcal{H}$-description, when satisfied with equality, determines a facet of the polytope.

Example 1.2.6. The cube P in Figure 1.2 has the following $\mathcal{H}$-description.

$$P := \left\{ (x_1, x_2) \in \mathbb{R}^2 \ : \ \begin{bmatrix} 1 & 0 \\ 0 & 1 \\ -1 & 0 \\ 0 & -1 \end{bmatrix} \begin{bmatrix} x_1 \\ x_2 \end{bmatrix} \leq \begin{bmatrix} 1 \\ 1 \\ 1 \\ 1 \end{bmatrix} \right\}$$

It is worth noting that, given a polytope, the fact that it has both $\mathcal{V}$- and $\mathcal{H}$-descriptions and a process for translating between the two are non-trivial to show [32, Section 1.1].

1.2.2   Some Properties of Interest

For any lattice polytope, there are many questions we can ask regarding its geometry and combinatorics.

Face Structure

Since every face of a polytope P is the intersection of P with some support hyperplane, we can further describe how faces "glue" together to create the boundary of the polytope. Namely,

- faces can intersect only at their boundaries,

- intersections of faces are faces,

- every face is attainable as an intersection of facets.

The *face vector* (or *f-vector*) and the *face lattice* of a polytope are invariants of a polytope that give information about the number of faces of each dimension and how faces are arranged.

3

Definition 1.2.7. For a d-dimensional polytope P, the *f-vector* is $f = (f_0, f_1, \ldots, f_{d-1})$ where f_i is the number of i-dimensional faces of P.

Definition 1.2.8. The *face lattice* of a polytope P is a partially ordered set where the elements are faces of P ordered by inclusion. In other words, if F and F' are faces of P, then $F \leq F'$ in the face lattice if $F \subseteq F'$ in the polytope. The minimal element of the face lattice is the empty face , and the maximal element is the entire polytope P.

Example 1.2.9. For a d-dimensional simplex, the f-vector has entries $f_i = \binom{d+1}{i+1}$, and the face lattice is the *boolean lattice* $\mathbb{B}_{d+1}$.

Remark 1.2.10. The f-vector and face lattice are both concepts that generalize to the study of *polytopal complexes*, geometric objects constructed by gluing polytopes along faces. When every polytope in a complex is a simplex, these are called *simplical complexes*, which are widely studied in algebraic combinatorics.

Additionally, every face of a polytope is itself a polytope, and anything we can ask about P (such as the questions that follow) can also be asked about faces of P.

Normalized Volume

As polytopes are geometric objects, we're often interested in understanding their volume.

Definition 1.2.11. For a d-dimensional polytope P, the *normalized volume* is defined

$$Vol(P) := d! \cdot vol(P)$$

where $vol(P)$ denotes the Euclidean volume of P.

Multiplying the Euclidean volume by $d!$ gives that the normalized volume of the standard simplex Δ_d is 1. We say that any simplex with normalized volume equal to 1 is a *unimodular simplex*.

In general, normalized volume is difficult to compute. For a lattice polytope P, we can sometimes make use of a relationship between $Vol(P)$ and the number of lattice points in dilates of P. This relationship and other questions surrounding lattice point enumeration are the focus of Ehrhart theory [1].

Definition 1.2.12. For a polytope $P \in \mathbb{R}^d$, the *lattice point enumerator* is the function

$$L_P(t) := |tP \cap \mathbb{Z}^d|,$$

which counts the integer points contained in the tth dilate of P.
The *Ehrhart series of P* is the generating function for $L_P(t)$, defined

$$\text{Ehr}_P(z) := 1 + \sum_{t \geq 1} L_P(t) z^t.$$

It has been shown that, for d-dimensional lattice polytopes, $L_P(t)$ is a polynomial in t and the Ehrhart series can be expressed as a rational function

$$\text{Ehr}_P(z) = \frac{\sum_{j=0}^{d} h_j^* z^j}{(1-z)^{d+1}}.$$

The numerator of this rational form of the Ehrhart series is called the h^*-*polynomial* of P, which is known to have coefficients that are nonnegative integers. Finding combinatorial interpretations of the h^* coefficients for families of lattice polytopes is an active area of study. One thing that is known is a connection with normalized volume.

Corollary 1.2.13. *For a d-dimensional lattice polytope P,*

$$Vol(P) = \sum_{j=0}^{d} h_j^*.$$

Triangulations

Like studying face structure tells us how the boundary of a polytope can be decomposed into simpler pieces, studying triangulations can tell us information about decomposing the polytope as a whole.

Definition 1.2.14. A *triangulation* of a d-dimensional polytope $P = \text{conv}\{v_1, \ldots, v_n\}$ is a subdivision of P into d-simplices $S_1, \ldots, S_k$ such that

- the vertices of S_i are in $\{v_1, \ldots, v_n\}$ for all i,

- $\bigcup_{i=1}^{k} S_i = P$,

- $S_i \cap S_j$ is a face of both S_i and S_j (possibly the empty face) for every i and j.

Some classical and well-studied examples are triangulations of a regular n-gon in $\mathbb{R}^2$, which are known to be counted by the Catalan numbers [28].

One nice family of triangulations for a given polytope are *regular* triangulations.

Definition 1.2.15. For a polytope $P = \text{conv}\{v_1, \ldots, v_n\} \in \mathbb{R}^d$, and a height function $\omega : \{v_1, \ldots, v_n\} \to \mathbb{R}$, a *regular subdivision* of P arises from ω by constructing the lifted polytope $P^\omega \in \mathbb{R}^{d+1}$ with vertices $\{(v_1, \omega(v_1)), \ldots, (v_n, \omega(v_n))\}$. The *lower faces* of P^ω are those that minimize a chosen linear functional. Projecting the lower faces of P^ω back to $\mathbb{R}^d$ gives the subdivision of P.

When all the lower faces of P^ω are simplices, we obtain a *regular triangulation*.

Example 1.2.16. Figure 1.3 illustrates the construction of a regular triangulation of a unit cube $P \subset \mathbb{R}^2$ (shown embedded into $\mathbb{R}^3$). The lower faces of P^ω (shown in green and purple in the figure) are the 2-simplices $\text{conv}\{(0,0,5), (1,0,5), (1,1,3)\}$ and $\text{conv}\{(0,0,5), (0,1,5), (1,1,3)\}$. These project to the simplices $\text{conv}\{(0,0), (1,0), (1,1)\}$ and $\text{conv}\{(0,0), (0,1), (1,1)\}$ in $\mathbb{R}^2$, which triangulate P.
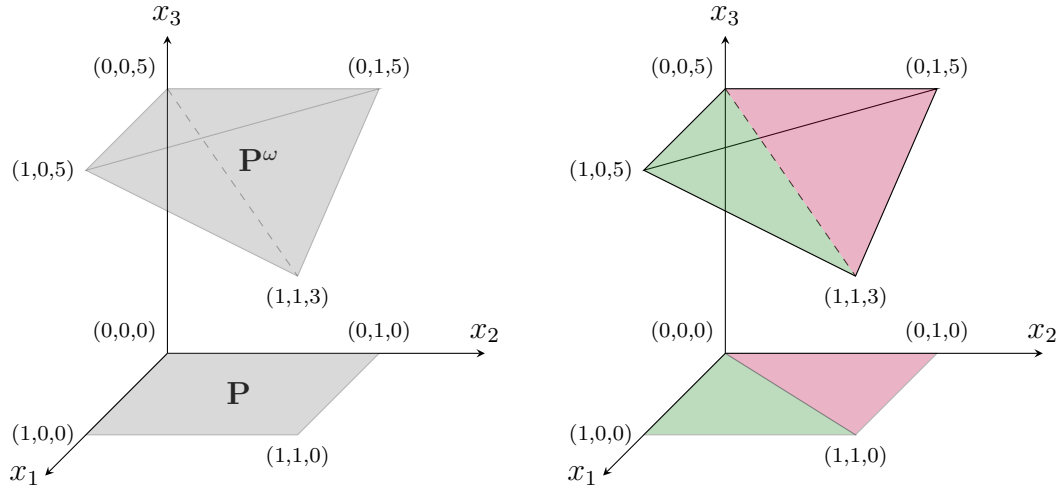
Figure 1.3: A regular triangulation of the unit cube $P \subset \mathbb{R}^2$.

It is fairly straightforward to obtain regular triangulations computationally, as they depend only on the choice of the height function and the linear functional that determines the lower faces.

Another desirable type of triangulation are *unimodular triangulations*, that is triangulations where the normalized volume of every simplex is 1. Though constructing unimodular triangulations still can be difficult, if we can find them for a given polytope P, the also difficult of question of computing $Vol(P)$ can be answered by counting the simplices in the triangulation.

Duals and Reflexivity

Given a collection of points (such as a polytope) in $\mathbb{R}^d$, we can construct its geometric dual'[32].

Definition 1.2.17. For $X \subseteq \mathbb{R}^d$, the *dual* (or *polar*) X^* of X is the set

$$X^* := \{z \in \mathbb{R}^d \ : \ z^T \cdot x \leq 1 \text{ for all } x \in X\}.$$

When our set X is actually a polytope P, we get a nice result.

Proposition 1.2.18. *If $P \subset \mathbb{R}^d$ is a d-dimensional polytope containing the origin in its interior, there is a bijection between facets of P and the vertices of P^*.*

Example 1.2.19. In any dimension d, the cube $[-1, 1]^d$ and $\text{conv}\{\pm e_i : i = 1, \dots, d\}$, the d-dimensional cross polytope are dual to each other. The 2-dimensional case is shown in Figure 1.4. We saw in Example 1.2.6 that the facets of the cube are defined by hyperplanes with (inward-pointing, unit) normal vectors that are exactly the vertices of the cross polytope. The same relationship can be verified for the facets of the cross polytope and the vertices of the cube.
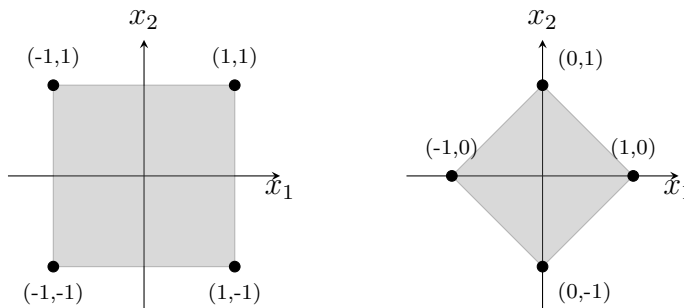
Figure 1.4: The $[-1, 1]$-cube and the cross polytope in $\mathbb{R}^2$. These polytopes are duals of each other. Thus both are reflexive.

In the example above, the dual of a lattice polytope was also a lattice polytope, which is not true in general. Lattice polytopes that have this property are called *reflexive*. We also have an alternate way to describe reflexive polytopes that makes this property very useful.

Definition 1.2.20. A lattice polytope P that contains the origin in its interior is *reflexive* if all of the facets of P are contained in hyperplanes that are lattice distance 1 from the origin. In other words, the $\mathcal{H}$-description of P can be expressed

$$P = \{\mathbf{x} \in \mathbb{R}^n \ : \ \mathbf{A}\mathbf{x} \leq \mathbf{1}\}$$

where $\mathbf{A} \in M^{k \times n}$ is a matrix with integer entries and $\mathbf{1} \in \mathbb{R}^k$ is the vector of all ones.

In any given dimension, there are finitely many reflexive lattice polytopes up to *unimodular equivalence* (a lattice-preserving transformation).

1.3 Graphs

A *graph* is a combinatorial structure often used to model relationships among collections of objects. Here we will restrict ourselves to a particular family of graphs.

Definition 1.3.1. A *simple, undirected graph* is a pair of sets, $G = (V, E)$

- V, a set of *vertices* (or nodes),

- E, a set of *edges*, unordered pairs of vertices.

Commonly, we will express a graph as a collection of dots representing the vertices and line segments representing the edges such as in Figure 1.5.

Throughout this work, we mainly concern ourselves with *connected* graphs, those in which there is a path of edges between any two vertices. A path of at least 3 edges that begins and ends at the same vertex is called a *cycle*. For example, the edges among vertices u, v, and w in Figure 1.5 form a cycle of length 3. A connected graph that contains no cycles is called a *tree*, and a graph that contains no cycles of odd length is called *bipartite*.

7
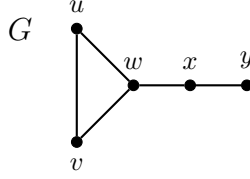
Figure 1.5: A simple, undirected graph G with vertex set $V = \{u, v, w, x, y\}$ and edge set $E = \{uv, uw, vw, wx, xy\}$.

While graphs are structures that store information about relationships, we can also use graphs to define and study other structures. Of particular interest in this work are polytopes that are defined from graphs.

1.4   Symmetric Edge Polytopes

Symmetric edge polytopes are a class of lattice polytopes defined from simple, undirected graphs that were introduced by Matsui, Higashitani, Nagazawa, Ohsugi, and Hibi in [19].

Definition 1.4.1. For a simple graph $G = (V, E)$, the *symmetric edge polytope* is defined

$$P_G := \text{conv}\{\pm(e_v - e_w) : vw \in E\} \subset \mathbb{R}^V,$$

where $e_v \in \mathbb{R}^V$ is the standard basis vector indexed by the vertex v of G.
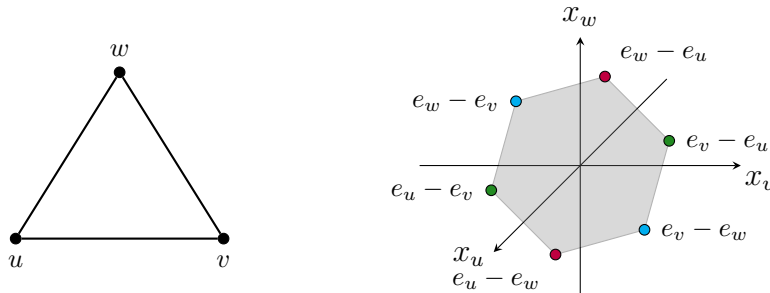
Figure 1.6: The complete graph K_3 (left) and it's symmetric edge polytope P_{K_3} (right), which is a 2-dimensional hexagon in $\mathbb{R}^3$.

Figure 1.6 demonstrates several properties that symmetric edge polytopes have in general. First, the symmetric edge polytope for a connected graph with n vertices is an $(n-1)$-dimensional polytope in $\mathbb{R}^n$. It is straightforward to see that any symmetric edge polytope is contained in the hyperplane $\sum_{i=1}^{n} x_i = 0$, the orthogonal complement of $\langle \mathbf{1} \rangle \subset \mathbb{R}^n$, the linear subspace spanned by the vector where every entry is one. Symmetric edge polytopes are also *centrally symmetric*, meaning that for every point $x \in P_G$, $-x$ is also in P_G. This also implies that every symmetric edge polytope

contains the origin. Finally, for any connected graph G with n vertices, P_G is reflexive with respect to the lattice $\mathbb{Z}^n/\langle \mathbf{1} \rangle$.

Symmetric edge polytopes (called *type PV adjacency polytopes* in some settings) have been the subject of intense recent study [6, 7, 8, 9, 10, 15, 18, 19, 23, 25]. In addition to investigating the interesting structure of these polytopes for its own sake, there are applications to the study of algebraic Kuramoto equations, systems of differential equations that model the behavior of coupled oscillators [7]. The relationships between the oscillators can be modeled by a graph, and it has been shown that the normalized volume of the symmetric edge polytope associated to that graph gives an upper bound on the number of solutions to the system. However, as discussed in Section 1.2.2, computing normalized volume can be a difficult or computationally costly task.

Unimodular triangulations are a tool that can assist in this case. Applying a result of Sturmfels, Higashitani, Jochemko, and Michałek [15] proved that symmetric edge polytopes have regular, unimodular triangulations. Still, counting the simplices of a unimodular triangulation is nontrivial. This process is aided by information about the number and volumes of facets in the polytope. The work of this thesis sits in this world– establishing formulas and bounds for the number of facets of symmetric edge polytopes in the service of finding information about triangulations and normalized volume.

Chapter 2 Facets of Symmetric Edge Polytopes for Graphs with Few Edges

In this chapter, we focus on the study the number of facets of P_G (hereafter denoted by $N(P_G)$ or $N(G)$) for connected graphs, with an emphasis on those graphs having few edges. This chapter is based on joint work with Benjamin Braun. A pre-print is available here [2].

Our study is motivated by the following questions: for a fixed number of vertices and edges, what properties of connected graphs lead to symmetric edge polytopes with either a large or small number of facets? This leads us to the following definition.

Definition 2.0.1. For $n \geq 2$ and $m \geq n-1$, define $maxf(n,m)$ to be the maximum number of facets of a symmetric edge polytope for a connected graph having n vertices and m edges, and similarly define $minf(n,m)$ to be the minimum number of facets. For $n \geq 2$, we define $Maxf(n)$ to be the maximum number of facets of a symmetric edge polytope for a connected graph having n vertices, and similarly define $Minf(n)$ to be the minimum number.

The first few values of $maxf(n,m)$, reserved as sequence A360408 in OEIS [17], are given in Table 2.1. The first few values of $minf(n,m)$, reserved as sequence A360409 in OEIS [17], are given in Table 2.2. The sequence $Maxf(n)$ is given by

$$2, 6, 14, 36, 84, 216, 504, 1296 \dots,$$

while the sequence $Minf(n)$ is given by

$$2, 4, 6, 10, 14, 22, 30, 46, \dots.$$

The problem of determining $maxf(n,m)$ and $minf(n,m)$ is challenging, in part due to the complicated combinatorial structures that describe the facets of P_G. Experimental data suggest that facet maximizing graphs can be obtained as a wedge product of odd cycles; how broadly this holds for general n and m beyond relatively sparse graphs is not clear. Computational evidence obtained with SageMath [29] leads to the following conjecture regarding the sequences $Maxf(n)$ and $Minf(n)$ (all undefined terms below are defined in subsequent sections).

Note that the conjectured sequence for $Minf(n)$ is entry A027383 in OEIS [16].

Conjecture 2.0.2. *Let $n \geq 3$.*

1. *For $n = 2k+1$, $Maxf(n) = 6^k$, which is attained by a wedge of k cycles of length three.*

2. *For $n = 2k$, $Maxf(n) = 14 \cdot 6^{k-1}$, which is attained by a wedge of K_4 with $k-1$ cycles of length three.*

3. *For $n = 2k+1$, $Minf(n) = 3 \cdot 2^k - 2$, which is attained by $K_{k,k+1}$.*

Table 2.1: $maxf(n,m)$.

$n, m-n+1$	0	1	2	3	4	5	6	7	8	9	10	11	12	13
2	2													
3	4	6												
4	8	12	12	14										
5	16	30	36	28	28	28	30							
6	32	60	72	72	84	68	68	60	60	60	62			
7	64	140	180	216	168	168	196	180	148	148	132	132	124	124

Table 2.2: $minf(n,m)$.

$n, m-n+1$	0	1	2	3	4	5	6	7	8	9	10	11	12	13	14	15
2	2															
3	4	6														
4	8	6	12	14												
5	16	12	10	22	26	28	30									
6	32	20	18	16	14	42	54	56	58	60	62					
7	64	40	32	28	26	24	22	78	102	106	116	118	120	122	124	126

4. For $n = 2k$, $Minf(n) = 2^{k+1} - 2$, which is attained by $K_{k,k}$.

Note that K_n denotes the *complete graph* with n vertices, and $K_{a,b}$ denotes the *complete bipartite graph* with shores of having a and b vertices, as shown in Figure 2.1.

Figure 2.1: Above are the complete graph K_4 (left), and the complete bipartite graph $K_{3,2}$ (right).

In this work, we investigate the sequences $maxf(n, n)$ and $maxf(n, n + 1)$. We provide an exact result for $maxf(n, n)$ and provide partial progress toward a conjectured value of $maxf(n, n + 1)$. The use of combinatorial tools for this analysis produces independently interesting integer sequences defined by sums of products of binomial coefficients.

2.1   Useful Tools and Known Results

It is known that the symmetric edge polytope for any tree on n vertices is combinatorially a cross polytope (meaning their face lattices are isomorphic) and thus has 2^{n-1} facets. Hence $maxf(n, n - 1) = 2^{n-1}$. More generally, the number of facets for symmetric edge polytopes can be derived using combinatorial tools. Specifically, a combinatorial description of the facet-defining hyperplanes of P_G was given by Higashitani, Jochemko, and Michałek [15]. Further, Chen, Davis, and Korchevskaia [6]

give a combinatorial description of the faces of P_G that utilizes special subgraphs of G.

Theorem 2.1.1 (Higashitani, Jochemko, Michałek [15]). *Let $G = (V, E)$ be a finite simple connected graph. Then $f : V \to \mathbb{Z}$ is facet-defining if and only if both of the following hold.*

(i) *For any edge $e = uv$ we have $|f(u) - f(v)| \leq 1$.*

(ii) *The subset of edges $E_f = \{e = uv \in E : |f(u) - f(v)| = 1\}$ forms a spanning connected subgraph of G.*

As symmetric edge polytopes are contained in the hyperplane orthogonal to the span of the vector of all ones, two facet-defining functions are identified if they differ by a common constant.

In other words, the facets of P_G are in bijection with these functions, which can be thought of as a special class of integer labelings of the vertices of G. Though counting these labelings is not particularly straightforward, this gives us our first significant tool.

The spanning connected subgraphs with edge sets E_f arising in Theorem 2.1.1, called *facet subgraphs*, also have further structure.

Lemma 2.1.2 (Chen, Davis, Korchevskaia [6]). *Let G be a connected graph. A subgraph H of G is a facet subgraph of G if and only if it is a maximal connected spanning bipartite subgraph of G.*

Lemma 2.1.2 provides a strategy for identifying the facets of P_G combinatorially: first identify the maximal connected spanning bipartite subgraphs of G, then determine the valid integer labelings of the vertices.

For a graph G that is constructed by identifying two graphs at a single vertex, there is a relationship between the facets of P_G and the facets of the subgraphs.

Definition 2.1.3. For graphs G and H, let $G \vee H$ denote a graph obtained by identifying a vertex in G with a vertex in H. We call $G \vee H$ a *wedge* or *join*.

Note that we do not specify a choice of identification points when defining $G \vee H$, as by the following proposition any such choice yields a symmetric edge polytope with the same number of facets.

Proposition 2.1.4. *For connected graphs G and H,*

$$N(P_{G \vee H}) = N(P_G) \cdot N(P_H).$$

Proof. This follows from the fact that $P_{G \vee H}$ is the free sum $P_G \oplus P_H$ [24, Proposition 4.2] (also called the direct sum) and the number of facets is multiplicative for free sums [14]. $\square$
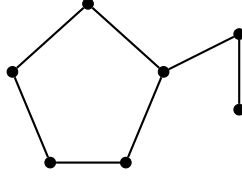
Figure 2.2: $C(7,5)$

Proposition 2.1.4 is particularly powerful when the graph we care about decomposes as a wedge of graphs for which facet counts of the symmetric edge polytopes are known. One known class of particular interest to us is cycles. Let C_n denote the cycle with n edges and let P_n denote the path with n edges.

Lemma 2.1.5. *For any m,*

$$N(P_{C_m}) = \begin{cases} \binom{m}{m/2} & m \ even \\ m\binom{m-1}{(m-1)/2} & m \ odd \end{cases}$$

Proof. For even m, the facets of P_{C_m} are identified and counted in [7, Proposition 12], and for odd m in [22, Remark 4.3]. $\square$

Though the two-cycle, C_2, is a multigraph (and thus, its symmetric edge polytope is not defined), its facet-defining functions would be exactly the facet-defining functions of a graph on two vertices with a single edge. This is consistent with the formula in Lemma 2.1.5.

2.2 Graphs With Few Edges and Disjoint Cycles

We consider the symmetric edge polytopes for classes of connected graphs where the number of edges is small relative to the number of vertices. We've previously stated that any tree T on n vertices has $N(T) = 2^{n-1}$ as P_T is combinatorially a cross polytope. With Proposition 2.1.4, we can see this another way. Any tree T can be constructed as a wedge of $n-1$ single edges with an appropriate choice of identification points, again giving $maxf(n, n-1) = 2^{n-1}$.

2.2.1 Graphs with n vertices and n edges

Considering next the sequence $maxf(n, n)$, any connected graph with an equal number of vertices and edges has a unique cycle, and hence can be constructed as a wedge of that cycle with trees. Therefore, we can count the facets of P_G for any such graph G and determine $maxf(n, n)$ for any n.

Definition 2.2.1. Let $C(n, m)$ denote a graph on n vertices obtained by joining an m-cycle with a path graph on $n - m$ edges.

13

Theorem 2.2.2. *For any connected graph G with n vertices and n edges, the number of facets of P_G is less than or equal to the number of facets of P_G for $G = C(n,n)$ when n is odd and $G = C(n, n-1)$ when n is even. Thus, for odd n*

$$maxf(n,n) = n \binom{n-1}{(n-1)/2},$$

and for even n

$$maxf(n,n) = 2(n-1) \binom{n-2}{(n-2)/2}.$$

Proof. A connected graph on n vertices and n edges has a unique cycle, C, of length m for some $3 \le m \le n$. Thus, G is the join of an m-cycle and $n - m$ edges. By Proposition 2.1.4, we have $N(G) = N(C(n,m))$. For $k \ge 2$, we claim

$$N(C(n,2k)) < N(C(n,2k-1)) < N(C(n,2k+1)). \tag{2.1}$$

In other words, if m is even, $N(C(n,m-1))$ is greater than $N(C(n,m))$. Also, if m is odd and $m \le n-2$, the graph $C(n, m+2)$ exists, and $N(C(n, m+2))$ is greater than $N(C(n,m))$. With these two statements, we see that $N(G)$ is maximized when G contains the largest odd cycle possible in a graph with n vertices.

To prove the inequality, let

$$\mathcal{M} = \frac{2^{n-(2k+1)}(2k-1)!}{(k!)^2}.$$

Then, by Lemma 2.1.5 and Proposition 2.1.4,

$$N(C(n,2k)) = N(C_{2k}) \cdot 2^{n-2k} = \binom{2k}{k} \cdot 2^{n-2k} = 4k\mathcal{M},$$

$$N(C(n,2k-1)) = N(C_{2k-1}) \cdot 2^{n-(2k-1)} = (2k-1)\binom{2k-2}{k-1} \cdot 2^{n-(2k-1)} = 4k^2\mathcal{M},$$

$$N(C(n,2k+1)) = N(C_{2k+1}) \cdot 2^{n-(2k+1)} = (2k+1)\binom{2k}{k} \cdot 2^{n-(2k+1)} = (4k^2 + 2k)\mathcal{M},$$

and the claim holds. $\qquad\square$

2.2.2 Graphs with n vertices and $n+1$ edges

We next consider the sequence $maxf(n, n+1)$, which is substantially more challenging than the previous cases. Any connected, simple graph with n vertices and $n+1$ edges can be constructed from a tree on n vertices by adding two edges. Each of these additions induces a cycle in the graph. For such graphs, we make the following definition and conjecture.
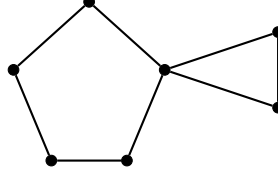
Figure 2.3: A graph with $N(G) = M(7)$

Definition 2.2.3. For $n \geq 3$, let $M(n)$ be the number of facets of P_G where

$$G := \begin{cases} C_{k+1} \vee C_{k-1} & n = 2k - 1, \ k \text{ even} \\ C_k \vee C_k & n = 2k - 1, \ k \text{ odd} \\ C_{k+1} \vee C_{k-1} \vee e & n = 2k, \ k \text{ even} \\ C_k \vee C_k \vee e & n = 2k, \ k \text{ odd} \end{cases}$$

Conjecture 2.2.4. *For all $n \geq 3$, $\max f(n, n+1)$ is equal to $M(n)$.*

Graphs with n vertices and $n+1$ edges fall into two categories: graphs with exactly 2 edge-disjoint cycles, such as those defined in Definition 2.2.6 below, and graphs where the cycles share one or more edges, such as those defined in Definition 2.3.2 below. In this section, we show that Conjecture 2.2.4 is true for the first category.

Theorem 2.2.5. *For any connected graph H with n vertices and $n + 1$ edges where H contains two edge-disjoint cycles, we have $N(H) \leq M(n)$.*

Note that Theorem 2.2.5 states that, among connected graphs with n vertices and $n + 1$ edges containing disjoint cycles, a facet-maximizing family arises by creating a graph that as closely as possible resembles the wedge of two equal-length odd cycles. The proof relies on the following definition and lemmas.

Definition 2.2.6. Let $G(n, i, j)$ denote the graph $C_i \vee C_j \vee P_{n+1-(i+j)}$. Note that $G(n, i, j)$ has n vertices and $n + 1$ edges.

Lemma 2.2.7. *If i is even, then*

$$N(G(n, i, j)) < N(G(n, i - 1, j)).$$

Proof. Note that $N(G(n, i, j)) = N(C(n+1-j, i) \vee C_j)$. Because i is even, applying the inequalities (2.1) and Proposition 2.1.4 yields

$$N(C(n + 1 - j, i) \vee C_j) < N(C(n + 1 - j, i - 1) \vee C_j) = N(G(n, i - 1, j)),$$

which completes the proof. $\square$

Lemma 2.2.8. *For i, j, m, ℓ odd with $m < i \leq j < \ell$ and $i + j = m + \ell$,*

$$N(C_m \vee C_\ell) < N(C_i \vee C_j).$$

Proof. We show this holds for $m = i - 2$ and $\ell = j + 2$, then the argument follows by induction. By Lemma 2.1.5 and Proposition 2.1.4

$$N(C_i \vee C_j) = ij \binom{i-1}{\frac{i-1}{2}} \binom{j-1}{\frac{j-1}{2}},$$

$$N(C_{i-2} \vee C_{j+2}) = (i-2)(j+2) \binom{i-3}{\frac{i-3}{2}} \binom{j+1}{\frac{j+1}{2}}.$$

Letting $\mathcal{M} = (i-2)j \binom{i-3}{\frac{i-3}{2}} \binom{j-1}{\frac{j-1}{2}}$, we see

$$N(C_{i-2} \vee C_{j+2}) = 4\mathcal{M} \cdot \frac{j+2}{j+1} < 4\mathcal{M} \cdot \frac{i}{i-1} = N(C_i \vee C_j).$$

$\square$

We also make use of the following theorem.

Theorem 2.2.9. *For all n*

$$2 \cdot M(n) \leq M(n+1).$$

Proof. By Lemma 2.1.5 and Proposition 2.1.4,

$$M(n) = \begin{cases} (k+1)(k-1)\binom{k}{\frac{k}{2}}\binom{k-2}{\frac{k-2}{2}} & n = 2k-1, \ k \text{ even} \\ k^2 \binom{k-1}{\frac{k-1}{2}}^2 & n = 2k-1, \ k \text{ odd} \\ 2 \cdot M(n-1) & n = 2k. \end{cases}$$

When n is odd, $2 \cdot M(n) = M(n+1)$, and we are done. When n is even, we consider two cases.

Case 1: If $n = 2k$ with k even, $n+1 = 2(k+1) - 1$ with $k+1$ odd. Therefore, letting $\mathcal{K} = (k+1)\binom{k}{\frac{k}{2}}$, we have

$$M(n) = 2 \cdot M(2k-1) = 2(k+1)(k-1)\binom{k}{\frac{k}{2}}\binom{k-2}{\frac{k-2}{2}} = 2(k-1)\binom{k-2}{\frac{k-2}{2}} \cdot \mathcal{K},$$

and

$$M(n+1) = (k+1)^2 \binom{k}{\frac{k}{2}}^2 = \mathcal{K}^2.$$

Since

$$\mathcal{K} = (k+1)\binom{k}{\frac{k}{2}} = \frac{(k+1)k}{\left(\frac{k}{2}\right)^2} \cdot (k-1) \cdot \binom{k-2}{\frac{k-2}{2}}$$

$$= \frac{4(k+1)}{k} \cdot (k-1) \cdot \binom{k-2}{\frac{k-2}{2}} \geq 4 \cdot (k-1) \cdot \binom{k-2}{\frac{k-2}{2}},$$

16

we see

$$2 \cdot M(n) = 4(k-1)\binom{k-2}{\frac{k-2}{2}} \cdot \mathcal{K} \leq \mathcal{K}^2 = M(n+1) \,.$$

Case 2: If $n = 2k$ with k odd, $n+1 = 2(k+1)-1$ with $k+1$ even. Therefore, letting $\mathcal{K} = k\binom{k-1}{\frac{k-1}{2}}$, we have

$$M(n) = 2 \cdot M(2k-1) = 2k^2 \binom{k-1}{\frac{k-1}{2}}^2 = 2\mathcal{K}^2$$

and

$$M(n+1) = (k+2)k\binom{k+1}{\frac{k+1}{2}}\binom{k-1}{\frac{k-1}{2}} = (k+2)\binom{k+1}{\frac{k+1}{2}} \cdot \mathcal{K} \,.$$

Since

$$(k+2)\binom{k+1}{\frac{k+1}{2}} = \frac{(k+2)(k+1)}{\left(\frac{k+1}{2}\right)^2} \cdot k \cdot \binom{k-1}{\frac{k-1}{2}} = \frac{4(k+2)}{(k+1)} \cdot \mathcal{K} \geq 4\mathcal{K}, \,,$$

we see

$$2 \cdot M(n) = 4\mathcal{K}^2 \leq (k+2)\binom{k+1}{\frac{k+1}{2}} \cdot \mathcal{K} = M(n+1) \,.$$

$\square$

With these in place, we have Theorem 2.2.5.

Proof of Theorem 2.2.5. By Proposition 2.1.4, any such graph H containing exactly two edge-disjoint cycles of length i and j satisfies $N(H) = N(G(n,i,j))$. Thus, it is sufficient to restrict our attention to $G(n,i,j)$. By Lemmas 2.2.7 and 2.2.8, we can consider only $G(n,i,j)$ for i,j odd and as close to $\frac{i+j}{2}$ as possible. Without loss of generality, suppose $i \leq j$.

Case 1: $n = 2k-1$, k *even.* Note that, since i and j are both odd, $i \leq k-1$ and $j \leq k+1$. Also, by Lemma 2.1.5 and Proposition 2.1.4,

$$N(G(n,i,j)) = 2^{n-(i+j)+1}ij\binom{i-1}{\frac{i-1}{2}}\binom{j-1}{\frac{j-1}{2}} = 2^{2k-(i+j)} \cdot \frac{i!j!}{\left(\frac{i-1}{2}!\right)^2\left(\frac{j-1}{2}!\right)^2} \,.$$

17

Similarly,

$$M(n) = (k+1)(k-1)\binom{k}{\frac{k}{2}}\binom{k-2}{\frac{k-2}{2}}$$

$$= \frac{(k+1)!}{\left(\frac{k}{2}!\right)^2} \cdot \frac{(k-1)!}{\left(\frac{k-2}{2}!\right)^2}$$

$$= \frac{j!}{\left(\frac{j-1}{2}!\right)^2} \cdot \left(\prod_{\substack{\ell=j+1 \\ \ell \text{ even}}}^{k} \frac{(\ell+1)\ell}{\left(\frac{\ell}{2}\right)^2}\right) \cdot \frac{i!}{\left(\frac{i-1}{2}!\right)^2} \cdot \left(\prod_{\substack{m=i+1 \\ m \text{ even}}}^{k-2} \frac{(m+1)m}{\left(\frac{m}{2}\right)^2}\right)$$

$$= 2^{2k-(i+j)} \cdot \frac{i!j!}{\left(\frac{i-1}{2}!\right)^2 \left(\frac{j-1}{2}!\right)^2} \cdot \left(\prod_{\substack{\ell=j+1 \\ \ell \text{ even}}}^{k} \frac{\ell+1}{\ell}\right) \cdot \left(\prod_{\substack{m=i+1 \\ m \text{ even}}}^{k-2} \frac{m+1}{m}\right)$$

$$\geq N(G(n,i,j)).$$

Case 2: $n = 2k-1$, k *odd.* Note that, by assumption, $i \leq k$ and $j \leq k$. Also, by Lemma 2.1.5 and Proposition 2.1.4,

$$N(G(n,i,j)) = 2^{n-(i+j)+1}ij\binom{i-1}{\frac{i-1}{2}}\binom{j-1}{\frac{j-1}{2}} = 2^{2k-(i+j)} \cdot \frac{i!j!}{\left(\frac{i-1}{2}!\right)^2 \left(\frac{j-1}{2}!\right)^2}.$$

Similarly,

$$M(n) = k^2\binom{k-1}{\frac{k-1}{2}}^2$$

$$= \frac{j!}{\left(\frac{j-1}{2}!\right)^2} \cdot \left(\prod_{\substack{\ell=j+1 \\ \ell \text{ even}}}^{k-1} \frac{(\ell+1)\ell}{\left(\frac{\ell}{2}\right)^2}\right) \cdot \frac{i!}{\left(\frac{i-1}{2}!\right)^2} \cdot \left(\prod_{\substack{m=i+1 \\ m \text{ even}}}^{k-1} \frac{(m+1)m}{\left(\frac{m}{2}\right)^2}\right)$$

$$= 2^{2k-(i+j)} \cdot \frac{i!j!}{\left(\frac{i-1}{2}!\right)^2 \left(\frac{j-1}{2}!\right)^2} \cdot \left(\prod_{\substack{\ell=j+1 \\ \ell \text{ even}}}^{k-1} \frac{\ell+1}{\ell}\right) \cdot \left(\prod_{\substack{m=i+1 \\ m \text{ even}}}^{k-1} \frac{m+1}{m}\right)$$

$$\geq N(G(n,i,j)).$$

Case 3: $n = 2k$. By Lemma 2.1.5 and Proposition 2.1.4,

$$N(G(n,i,j)) = 2^{n-(i+j)+1}ij\binom{i-1}{\frac{i-1}{2}}\binom{j-1}{\frac{j-1}{2}} = 2 \cdot N(G(n-1,i,j)).$$

Also, by Theorem 2.2.9 and the previous cases,

$$M(n) \geq 2 \cdot M(n-1)$$
$$\geq 2 \cdot N(G(n-1,i,j))$$
$$= N(G(n,i,j)).$$

Thus, in every case, $N(G(n,i,j)) \leq M(n)$. □

So we are able to verify that Conjecture 2.2.4 holds in cases when the cycles in our graph do not share edges. Section 2.3 discusses what happens when they do.

2.3 Graphs with Few Edges and Overlapping Cycles

We next consider the family of graphs on n vertices and $n + 1$ edges that have two cycles intersecting in at least one edge. Theorem 2.2.9 allows us to reduce Conjecture 2.2.4 to the case where G has no vertices of degree one, as follows.

Corollary 2.3.1. *If Conjecture 2.2.4 is true for graphs on n vertices, then it is true for graphs on $n + 1$ vertices that have at least one leaf.*

Proof. Let G be a graph on $n+1$ vertices and $n+2$ edges that has a leaf e. Then $G\backslash\{e\}$ is a graph with n vertices and $n + 1$ edges, and by assumption $N(G \setminus \{e\}) \leq M(n)$. By Proposition 2.1.4 and Theorem 2.2.9,

$$N(G) = 2 \cdot N(G \setminus \{e\}) \leq 2 \cdot M(n) \leq M(n + 1).$$

$\square$

Corollary 2.3.1 allows us to restrict our attention to graphs with no leaves. Any graph on n vertices and $n + 1$ edges with no leaves that contains cycles sharing one or more edges can be interpreted as three internally disjoint paths connected at their endpoints. We consider these as a special case of a more general construction.

Definition 2.3.2. For a vector $\mathbf{m} \in \mathbb{N}^t$, let $CB(\mathbf{m})$ denote the graph made of t internally disjoint paths of lengths $m_1, m_2, \ldots, m_t$ connecting two endpoints.

Note that when $t = 3$, we obtain the leafless connected graphs with n vertices and $n + 1$ edges. Also, the graphs $CB(\mathbf{m})$ for which all entries of $\mathbf{m}$ are the same $m \in \mathbb{N}$ are sometimes called *theta graphs*, denoted by $\theta_{m,t}$ [11].

Proposition 2.3.3. *For $\mathbf{m} \in \mathbb{N}^t$, we may permute the entries so that without loss of generality we have $m_1 \geq m_2 \geq \cdots \geq m_t$. If all the m_i's have the same parity, $N(CB(\mathbf{m}))$ is given by*

$$F(\mathbf{m}) = \sum_{j=0}^{m_t} \binom{m_t}{j} \left[\prod_{k=1}^{t-1} \binom{m_k}{\frac{1}{2}(m_k - m_t) + j} \right].$$

Proof. Consider $CB(\mathbf{m})$ as consisting of paths $P_1, P_2, \ldots, P_t$ having $m_1 \geq \cdots \geq m_t$ edges respectively, as shown in Figure 2.4. Since all m_i are the same parity, $CB(\mathbf{m})$ is bipartite. By [9, Lem. 4.5], for every facet-defining function $f : V \to \mathbb{Z}$, we have $|f(u) - f(v)| = 1$ for every edge uv in $CB(\mathbf{m})$. If we consider the paths as oriented away from the top vertex toward the bottom vertex, we can view each edge $u \to v$ as ascending ($f(v) - f(u) = 1$), and label it 1, or descending ($f(v) - f(u) = -1$), and label it -1.

We count facets by finding *valid* labelings of the edges of $CB(\mathbf{m})$ with ± 1, that is labelings such that the sum of the labels on every path is the same. For a labeling of a shortest path with length m_t using j -1s and $m_t - j$ 1s, the sum of the edge labels is $m_t - 2j$. There are $\binom{m_t}{j}$ labelings of this path with this sum.
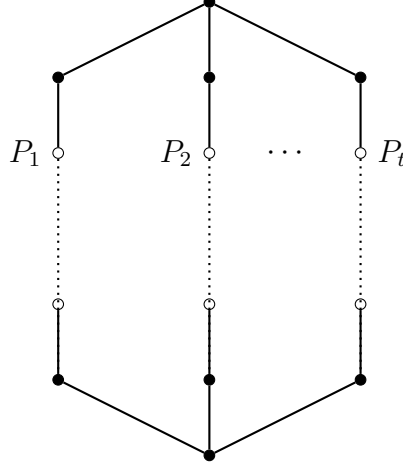
Figure 2.4: $CB(\mathbf{m})$ for $\mathbf{m} = (m_1, \ldots, m_t)$

To produce a valid labeling of the entire graph with each path sum equal to $m_t - 2j$, the number of -1s, say y, on a path of length m_k must satisfy the equation:

$$(+1)(m_k - y) + (-1)y = m_t - 2j$$

$$y = \frac{1}{2}(m_k - m_t) + j.$$

Thus there are $\binom{m_k}{\frac{1}{2}(m_k - m_t) + j}$ labelings of a path of length m_k with label sum $m_t - 2j$. Applying this argument to m_k for $k = 1, \ldots, t-1$ gives

$$\binom{m_t}{j} \prod_{k=1}^{t-1} \binom{m_k}{\frac{1}{2}(m_k - m_t) + j}$$

valid labelings of $CB(\mathbf{m})$ with j -1s on the shortest path. The result follows by taking the sum over all $j = 0, \ldots, m_t$. $\qquad\square$

Note that there is a combinatorial interpretation for F, where we consider the arithmetical triangle of binomial coefficients vertically centered at the central terms. What F does is select the m_t-th row of the arithmetical triangle, multiply each entry by the vertically-aligned entries in rows m_1 through m_{t-1}, and sum the resulting products.

For $CB(\mathbf{m}) = \theta_{m,t}$ where all the paths are the same length, this formula simplifies.

Corollary 2.3.4. *For $t \in \mathbb{N}$,*

$$N(\theta_{m,t}) = \sum_{j=0}^{m} \binom{m}{j}^t.$$

If the vector $\mathbf{m}$ has both even and odd entries, counting the facets of $CB(\mathbf{m})$ becomes more complicated, but still involves F.

Proposition 2.3.5. *For* $\mathbf{m} \in \mathbb{N}^t$, *permute the entries so that* $\mathbf{m} = (e_1, \ldots, e_k, o_1, \ldots, o_\ell)$ *with* $e_1 \geq e_2 \geq \cdots \geq e_k$ *even and* $o_1 \geq o_2 \geq \cdots \geq o_\ell$ *odd and* $k, \ell \geq 1$, $k + \ell = t$. *Also, let* $\mathbf{m}_e$ *be the vector obtained by subtracting* 1 *from every even entry of* $\mathbf{m}$, *and* $\mathbf{m}_o$ *the vector obtained by subtracting* 1 *from every odd entry of* $\mathbf{m}$.

(i) *If all entries of* $\mathbf{m}$ *are at least* 2,

$$N(CB(\mathbf{m})) = \left(\prod_{j=1}^{k} e_j\right) F(\mathbf{m}_e) + \left(\prod_{j=1}^{\ell} o_j\right) F(\mathbf{m}_o).$$

(ii) *If* $o_{p+1} = \cdots = o_\ell = 1$ *(and* $o_p > 1$),

$$N(CB(\mathbf{m})) = \left(\prod_{j=1}^{k} e_j\right) F(\mathbf{m}_e) + \left(\prod_{j=1}^{\ell} o_j\right) N\left(\left(\vee_{j=1}^{k} C_{e_j}\right) \vee \left(\vee_{j=1}^{p} C_{o_j-1}\right)\right).$$

Proof. Consider $CB(\mathbf{m})$ as in Figure 2.4. As in the proof of Proposition 2.3.3, we will count facets of $P_{CB(\mathbf{m})}$ by counting valid labelings of the facets subgraphs of $CB(\mathbf{m})$. These subgraphs are those in which

1. one edge of every even length path has been removed, or

2. one edge of every odd length path has been removed.

We can view these as labelings of $CB(\mathbf{m})$ where the sum of labels on each P_i is equal, and all edges must be labeled with ± 1 except

1. one edge on each even path is labeled 0, or

2. one edge on each odd path is labeled 0.

In (1), there are $\prod_{j=1}^{k} e_j$ ways to choose the edges to label 0. Having the edge uv labeled 0 indicates that $f(u) = f(v)$ in the corresponding facet-defining function $f : V \to \mathbb{Z}$. Thus, we can view this edge as having been contracted since its endpoints have the same value. Then the reduced graph with these edges contracted is $CB(\mathbf{m}_e)$, constructed of paths that all have odd length. So, by Proposition 2.3.3, the number of valid labelings of $CB(\mathbf{m})$ where each even path has a 0 edge is

$$\left(\prod_{j=1}^{k} e_j\right) F(\mathbf{m}_e).$$

In (2), there are $\prod_{j=1}^{\ell} o_j$ ways to choose the edges to label 0. If every entry of $\mathbf{m}$ is at least 2, the graph produced by contracting these 0 edges is $CB(\mathbf{m}_o)$, constructed

21

of paths that all have even length. As above, the number of valid labelings of $CB(\mathbf{m})$ of this type is

$$\left(\prod_{j=1}^{\ell} o_j\right) F(\mathbf{m}_o).$$

Thus, in case (i),

$$N(CB(\mathbf{m})) = \left(\prod_{j=1}^{k} e_j\right) F(\mathbf{m}_e) + \left(\prod_{j=1}^{\ell} o_j\right) F(\mathbf{m}_o).$$

To complete case (ii), note that if we contract any edge on a path of length 1, the endpoints of the remaining paths are identified, and the reduced graph is a wedge of cycles. In particular, if $o_{p+1} = \cdots = o_\ell = 1$ and $o_p > 1$, the reduced graph is $\left(\vee_{j=1}^{k} C_{e_j}\right) \vee \left(\vee_{j=1}^{p} C_{o_j-1}\right)$. So the number of valid labelings of $CB(\mathbf{m})$ of this type is

$$N\left(\left(\vee_{j=1}^{k} C_{e_j}\right) \vee \left(\vee_{j=1}^{p} C_{o_j-1}\right)\right).$$

Therefore, in case (ii),

$$N(CB(\mathbf{m})) = \left(\prod_{j=1}^{k} e_j\right) F(\mathbf{m}_e) + \left(\prod_{j=1}^{\ell} o_j\right) N\left(\left(\vee_{j=1}^{k} C_{e_j}\right) \vee \left(\vee_{j=1}^{p} C_{o_j-1}\right)\right).$$

$\square$

Returning to the special case of leafless connected graphs on n vertices with $n+1$ edges, specializing to $t = 3$ provides facet counts for our graphs of interest.

Corollary 2.3.6. *The number of facets of the symmetric edge polytope for $CB(x_1, x_2, x_3)$ is computed as follows.*

(i) For x_1, x_2, x_3 either all even or all odd,

$$N(CB(x_1, x_2, x_3)) = F(x_1, x_2, x_3).$$

(ii) For o_1, o_2 odd, e_1 even, and all at least 2,

$$N(CB(o_1, o_2, e_1)) = e_1 F(o_1, o_2, e_1 - 1) + o_1 o_2 F(o_1 - 1, o_2 - 1, e_1).$$

For e_1, e_2 even, o_1 odd, and all at least 2,

$$N(CB(e_1, e_2, o_1)) = o_1 F(e_1, e_2, o_1 - 1) + e_1 e_2 F(e_1 - 1, e_2 - 1, o_1).$$

(iii) For e_1, e_2 even, and $o_1 = 1$,

$$N(CB(e_1, e_2, 1)) = e_1 e_2 F(e_1 - 1, e_2 - 1, 1) + N(C_{e_1} \vee C_{e_2})$$
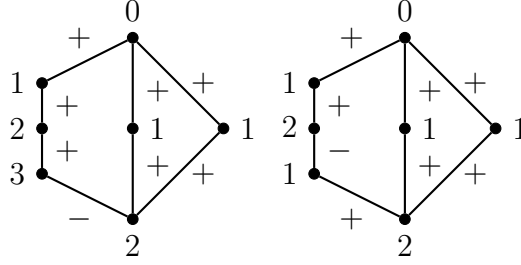
Figure 2.5: Some of the facet-defining functions of $CB(4,2,2)$ when $j = 0$
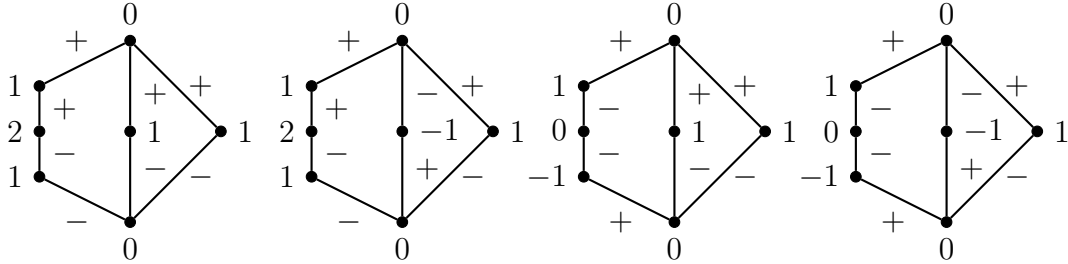
Figure 2.6: Some of the facet-defining functions of $CB(4,2,2)$ when $j = 1$
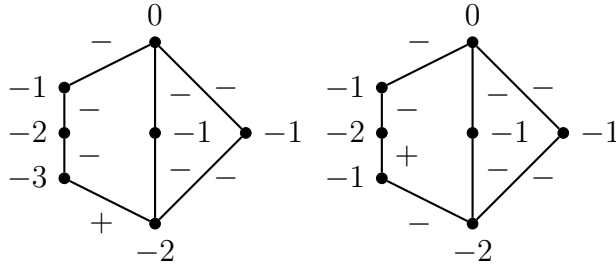
Figure 2.7: Some of the facet-defining functions of $CB(4,2,2)$ when $j = 2$

(iv) For e_1 even, $o_1 \geq 3$ odd,

$$N(CB(e_1, o_1, 1)) = e_1 F(e_1 - 1, o_1, 1) + o_1 N(C_{o_1-1} \vee C_{e_1})$$

(v) For e_1 even,
$$N(CB(e_1, 1, 1)) = e_1 F(e_1 - 1, 1, 1) + N(C_{e_1})$$

Example 2.3.7. Figures 2.5, 2.6, and 2.7 illustrate some of the facet-defining functions for the symmetric edge polytope of $CB(4, 2, 2)$. The vertices are labeled with their function values, and the edges are labeled " $+$ " if they're ascending and " $-$ " if they're descending.

Using these results, we can make partial progress toward Conjecture 2.2.4 in two special cases, given below in Theorem 2.3.8 and Proposition 2.3.10.

23

Theorem 2.3.8. *For all $n \geq 4$, if $x_1 \geq x_2 \geq x_3 \geq 1$, all x_i's have the same parity, and $x_1 + x_2 + x_3 = n + 1$, then*

$$F(x_1, x_2, x_3) \leq M(n).$$

Thus, if x_1, x_2, x_3 are all of the same parity, then Conjecture 2.2.4 is true.

Remark 2.3.9. The proof of Theorem 2.3.8 makes use of the Stirling bounds on $n!$ given in [26]. Namely,

$$\sqrt{2\pi}\, n^{n+\frac{1}{2}} e^{-n} e^{\frac{1}{12n+1}} \leq n! \leq \sqrt{2\pi}\, n^{n+\frac{1}{2}} e^{-n} e^{\frac{1}{12n}}.$$

Proof of Theorem 2.3.8. In each of the following cases, we show that the desired inequality holds for large enough n. For all smaller values of n we have verified that the theorem holds using SageMath [29]. Throughout the proof, we use the notation $\overset{!}{\leq}$ to indicate an unproven inequality we wish to show.

Case 1 ($n = 2k - 1$): In this case, $x_1 + x_2 + x_3 = 2k$, and all x_i's are even by assumption. Then we have:

$$F(x_1, x_2, x_3) = \sum_{j=0}^{x_3} \binom{x_3}{j} \binom{x_2}{\frac{1}{2}(x_2 - x_3) + j} \binom{x_1}{\frac{1}{2}(x_1 - x_3) + j}$$

$$\leq (x_3 + 1) \binom{x_3}{\frac{x_3}{2}} \binom{x_2}{\frac{x_2}{2}} \binom{x_1}{\frac{x_1}{2}}$$

Subcase 1(a): If k is even,

$$M(n) = M(2k - 1) = (k+1)(k-1) \binom{k}{\frac{k}{2}} \binom{k-2}{\frac{k-2}{2}}.$$

In this case, to show $F(x_1, x_2, x_3) \leq M(n)$, it suffices to show

$$(x_3 + 1)x_3!x_2!x_1! \left(\frac{k}{2}!\right)^2 \left(\frac{k-2}{2}!\right)^2 \overset{!}{\leq} (k+1)(k-1)k!(k-2)! \left(\frac{x_3}{2}!\right)^2 \left(\frac{x_2}{2}!\right)^2 \left(\frac{x_1}{2}!\right)^2 \tag{2.2}$$

By the Stirling bounds on $n!$, it suffices to show

$$\left(\begin{array}{c} (x_3 + 1)x_3^{x_3+\frac{1}{2}} x_2^{x_2+\frac{1}{2}} x_1^{x_1+\frac{1}{2}} \\[4pt] \cdot \left(\frac{k}{2}\right)^{k+1} \left(\frac{k-2}{2}\right)^{k-1} \\[4pt] \cdot e^{-(x_1+x_2+x_3+2k)+2} \\[4pt] \cdot e^{\frac{1}{12x_3}+\frac{1}{12x_2}+\frac{1}{12x_1}+\frac{1}{3k}+\frac{1}{3(k-2)}} \end{array} \right) \overset{!}{\leq} \left(\begin{array}{c} \sqrt{2\pi} \left(\frac{x_3}{2}\right)^{x_3+1} \left(\frac{x_2}{2}\right)^{x_2+1} \left(\frac{x_1}{2}\right)^{x_1+1} \\[4pt] \cdot (k+1)(k-1)k^{k+\frac{1}{2}}(k-2)^{k-\frac{3}{2}} \\[4pt] \cdot e^{-(x_1+x_2+x_3+2k)+2} \\[4pt] \cdot e^{\frac{1}{12k+1}+\frac{1}{12k-23}+\frac{2}{6x_3+1}+\frac{2}{6x_2+1}+\frac{2}{6x_1+1}} \end{array} \right)$$

24

or equivalently,

$$
\begin{pmatrix}
(x_3 + 1) \\
\cdot k^{k+1}(k-2)^{k-1} \\
\cdot e^{\frac{1}{12x_3} + \frac{1}{12x_2} + \frac{1}{12x_1} + \frac{1}{3k} + \frac{1}{3(k-2)}}
\end{pmatrix}
\overset{!}{\le}
\begin{pmatrix}
\frac{\sqrt{2\pi}}{8}\sqrt{x_1 x_2 x_3} \\
\cdot (k+1)(k-1)k^{k+\frac{1}{2}}(k-2)^{k-\frac{3}{2}} \\
\cdot e^{\frac{1}{12k+1} + \frac{1}{12k-23} + \frac{2}{6x_3+1} + \frac{2}{6x_2+1} + \frac{2}{6x_1+1}}
\end{pmatrix}.
$$

Since $\frac{1}{12k+1} + \frac{1}{12k-23} > 0$ for $k \ge 2$,

$$
e^{\frac{1}{12k+1} + \frac{1}{12k-23}} > 1.
$$

Also,

$$
-1 \le \frac{1}{12x} - \frac{2}{6x+1} \le 0
$$

for all $x \ge 1$ and so

$$
0 \le e^{\frac{1}{12x_3} - \frac{2}{6x_3+1} + \frac{1}{12x_2} - \frac{2}{6x_2+1} + \frac{1}{12x_1} - \frac{2}{6x_1+1}} \le 1
$$

for all x_1, x_2, x_3. Therefore, to show inequality (2.2), it suffices to show

$$
(x_3 + 1)k^{k+1}(k-2)^{k-1}e^{\frac{1}{3k} + \frac{1}{3(k-2)}} \overset{!}{\le} \frac{\sqrt{2\pi}}{8}(k+1)(k-1)k^{k+\frac{1}{2}}(k-2)^{k-\frac{3}{2}}\sqrt{x_1 x_2 x_3}
$$

or rather,

$$
(x_3 + 1)\sqrt{k(k-2)}e^{\frac{1}{3k} + \frac{1}{3(k-2)}} \overset{!}{\le} \frac{\sqrt{2\pi}}{8}(k+1)(k-1)\sqrt{x_1 x_2 x_3}
$$

Finally, we note the following:

- By assumption, $x_3 + 1 \le \frac{2k}{3} + 1 \le k + 1$, and so $\frac{x_3 + 1}{k + 1} \le 1$.

- $\frac{\sqrt{k(k-2)}}{k - 1} \le 1$.

- $0 < e^{\frac{1}{3k} + \frac{1}{3(k-2)}} < e$ for $k \ge 3$.

- By assumption, $x_1 \ge \frac{2k}{3}$, and $x_2, x_3 \ge 2$, implying $x_1 x_2 x_3 \ge \frac{8k}{3}$.

With this, it suffices to show

$$
e \le \frac{\sqrt{2\pi}}{8}\sqrt{\frac{8k}{3}}
$$

or

$$
k \ge \frac{12e^2}{\pi} \approx 28.224.
$$

25

This inequality and the desired inequality hold for all even $k \geq 30$.

Subcase 1(b): If k is odd,

$$M(n) = M(2k-1) = k^2 \binom{k-1}{\frac{k-1}{2}}.$$

To show $F(x_1, x_2, x_3) \leq M(n)$, it suffices to show

$$(x_3+1)\, x_3! x_2! x_1! \left(\frac{k-1}{2}!\right)^4 \overset{!}{\leq} (k!)^2 \left(\frac{x_3}{2}!\right)^2 \left(\frac{x_2}{2}!\right)^2 \left(\frac{x_1}{2}!\right)^2. \qquad (2.3)$$

By the Stirling bounds on $n!$, it suffices to show

$$\left(\begin{array}{c} (x_3+1)x_3^{x_3+\frac{1}{2}} x_2^{x_2+\frac{1}{2}} x_1^{x_1+\frac{1}{2}} \\[4pt] \cdot \left(\frac{k-1}{2}\right)^{2k} \\[4pt] \cdot e^{-(x_1+x_2+x_3+2k)+2} \\[4pt] \cdot e^{\frac{1}{12x_3}+\frac{1}{12x_2}+\frac{1}{12x_1}+\frac{2}{3(k-1)}} \end{array}\right) \overset{!}{\leq} \left(\begin{array}{c} \sqrt{2\pi} \left(\frac{x_3}{2}\right)^{x_3+1} \left(\frac{x_2}{2}\right)^{x_2+1} \left(\frac{x_1}{2}\right)^{x_1+1} \\[4pt] \cdot k^{2k+1} \\[4pt] \cdot e^{-(x_1+x_2+x_3+2k)} \\[4pt] \cdot e^{\frac{2}{12k+1}+\frac{2}{6x_3+1}+\frac{2}{6x_2+1}+\frac{2}{6x_1+1}}. \end{array}\right)$$

Using the same kinds of computations as the previous case, we see it suffices to show

$$e^2 (x_3+1)(k-1)^{2k} e^{\frac{2}{3(k-1)}} \overset{!}{\leq} \frac{\sqrt{2\pi}}{8} k^{2k+1} \sqrt{x_1 x_2 x_3}$$

Now note that:

- $x_3 + 1 \leq \dfrac{2k}{3} + 1 \leq k$ for $k \geq 3$, and so $\frac{x_3+1}{k} \leq 1$.

- $e^2 \left(\dfrac{k-1}{k}\right)^{2k} \leq 1$ for $k \geq 3$.

- $1 \leq e^{\frac{2}{3(k-1)}} \leq e$ for $k \geq 2$.

So, it suffices to show

$$e \overset{!}{\leq} \frac{\sqrt{2\pi}}{8}\sqrt{x_1 x_2 x_3},$$

which, as before, holds for

$$k \geq \frac{12e^2}{\pi} \approx 28.224$$

or all odd $k \geq 29$.

Case 2 ($n = 2k$): In this case, $x_1 + x_2 + x_3 = 2k + 1$, and all x_i's are odd by assumption. Then,

$$F(x_1, x_2, x_3) = \sum_{j=0}^{x_3} \binom{x_3}{j} \binom{x_2}{\frac{1}{2}(x_2 - x_3) + j} \binom{x_1}{\frac{1}{2}(x_1 - x_3) + j}$$

$$\leq (x_3 + 1) \binom{x_3}{\frac{x_3 - 1}{2}} \binom{x_2}{\frac{x_2 - 1}{2}} \binom{x_1}{\frac{x_1 - 1}{2}}$$

Subcase 2(a): If k is even,

$$M(n) = M(2k) = 2(k + 1)(k - 1) \binom{k}{\frac{k}{2}} \binom{k - 2}{\frac{k-2}{2}}.$$

To show $F(x_1, x_2, x_3) \leq M(n)$, it suffices to show

$$(x_3 + 1)\, x_3! x_2! x_1! \left(\frac{k}{2}!\right)^2 \left(\frac{k - 2}{2}!\right)^2 \overset{!}{\leq}$$

$$2(k + 1)(k - 1)k!(k - 2)! \left(\frac{x_3 - 1}{2}!\right) \left(\frac{x_3 + 1}{2}!\right) \left(\frac{x_2 - 1}{2}!\right) \left(\frac{x_2 + 1}{2}!\right) \left(\frac{x_1 - 1}{2}!\right) \left(\frac{x_1 + 1}{2}!\right).$$

$$(2.4)$$

Equivalently,

$$(x_3 + 1)\, x_3! x_2! x_1! \left(\frac{k}{2}!\right)^2 \left(\frac{k - 2}{2}!\right)^2 \overset{!}{\leq}$$

$$2(k + 1)(k - 1)k!(k - 2)! \left(\frac{x_3 + 1}{2}!\right)^2 \left(\frac{x_2 + 1}{2}!\right)^2 \left(\frac{x_1 + 1}{2}!\right)^2 \left(\frac{8}{(x_3 + 1)(x_2 + 1)(x_1 + 1)}\right),$$

or

$$(x_3 + 1)\, (x_3 + 1)!(x_2 + 1)!(x_1 + 1)! \left(\frac{k}{2}!\right)^2 \left(\frac{k - 2}{2}!\right)^2 \overset{!}{\leq}$$

$$16(k + 1)(k - 1)k!(k - 2)! \left(\frac{x_3 + 1}{2}!\right)^2 \left(\frac{x_2 + 1}{2}!\right)^2 \left(\frac{x_1 + 1}{2}!\right)^2.$$

By the Stirling bounds, it suffices to show

$$
\left(
\begin{array}{c}
(x_3+1)(x_3+1)^{x_3+\frac{3}{2}}(x_2+1)^{x_2+\frac{3}{2}}(x_1+1)^{x_1+\frac{3}{2}} \\[2mm]
\cdot\left(\frac{k}{2}\right)^{k+1}\left(\frac{k-2}{2}\right)^{k-1} \\[2mm]
\cdot e^{-(x_3+x_2+x_1+2k+1)} \\[2mm]
\cdot e^{\frac{1}{12(x_3+1)}+\frac{1}{12(x_2+1)}+\frac{1}{12(x_1+1)}+\frac{1}{3k}+\frac{1}{3(k-2)}}
\end{array}
\right)
\overset{!}{\leq}
$$

$$
\left(
\begin{array}{c}
16\sqrt{2\pi}\left(\frac{x_3+1}{2}\right)^{x_3+2}\left(\frac{x_2+1}{2}\right)^{x_2+2}\left(\frac{x_1+1}{2}\right)^{x_1+2} \\[2mm]
\cdot(k+1)(k-1)k^{k+\frac{1}{2}}(k-1)^{k-\frac{3}{2}} \\[2mm]
\cdot e^{-(x_3+x_2+x_1+2k+1)} \\[2mm]
\cdot e^{\frac{1}{12k+1}+\frac{1}{12(k-2)+1}+\frac{2}{6(x_3+1)+1}+\frac{2}{6(x_2+1)+1}+\frac{2}{6(x_1+1)+1}}
\end{array}
\right)
$$

After computations similar to those in Case 1, we see it suffices to show

$$
(x_3+1)\sqrt{k(k-2)}e \overset{!}{\leq} \frac{\sqrt{2\pi}}{8}(k+1)(k-1)\sqrt{(x_1+1)(x_2+1)(x_3+1)}
$$

where $x_1+1 \geq \frac{2k+4}{3}$, $x_2+1 \geq 2$, $x_3+1 \geq 2$. It suffices to have

$$
e \overset{!}{\leq} \frac{\sqrt{2\pi}}{8}\sqrt{4\left(\frac{2k+4}{3}\right)}
$$

or

$$
k \geq \frac{12e^2}{\pi} - 2 \approx 26.224.
$$

So the desired inequality holds for even $k \geq 28$.

Subcase 2(b): If k is odd,

$$
M(n) = M(2k) = 2k^2\left(\frac{k-1}{\frac{k-1}{2}}\right)^2
$$

To show $F(x_1, x_2, x_3) \leq M(n)$ it suffices to show

$$
(x_3+1)x_3!x_2!x_1!\left(\frac{k-1}{2}!\right)^4 \overset{!}{\leq}
$$
$$
2(k!)^2\left(\frac{x_3-1}{2}!\right)\left(\frac{x_3+1}{2}!\right)\left(\frac{x_2-1}{2}!\right)\left(\frac{x_2+1}{2}!\right)\left(\frac{x_1-1}{2}!\right)\left(\frac{x_1+1}{2}!\right).
\tag{2.5}
$$

Equivalently,

$$(x_3 + 1)\, x_3!x_2!x_1! \left(\frac{k-1}{2}!\right)^4 \overset{!}{\leq}$$

$$2(k!)^2 \left(\frac{x_3+1}{2}!\right)^2 \left(\frac{x_2+1}{2}!\right)^2 \left(\frac{x_1+1}{2}!\right)^2 \left(\frac{8}{(x_3+1)(x_2+1)(x_1+1)}\right),$$

or

$$(x_3+1)(x_3+1)!(x_2+1)!(x_1+1)!\left(\frac{k-1}{2}!\right)^4 \overset{!}{\leq}$$

$$16(k!)^2 \left(\frac{x_3+1}{2}!\right)^2 \left(\frac{x_2+1}{2}!\right)^2 \left(\frac{x_1+1}{2}!\right)^2$$

By the Stirling bounds, it suffices to show

$$\left(\begin{array}{c} (x_3+1)(x_3+1)^{x_3+\frac{3}{2}}(x_2+1)^{x_2+\frac{3}{2}}(x_1+1)^{x_1+\frac{3}{2}} \\[2mm] \cdot \left(\frac{k-1}{2}\right)^{2k} \\[2mm] \cdot e^{-(x_3+x_2+x_1+2k+1)} \\[2mm] \cdot e^{\frac{1}{12(x_3+1)}+\frac{1}{12(x_2+1)}+\frac{1}{12(x_1+1)}+\frac{2}{3(k-1)}} \end{array} \right) \overset{!}{\leq}$$

$$\left(\begin{array}{c} 16\sqrt{2\pi}\ \left(\frac{x_3+1}{2}\right)^{x_3+2}\left(\frac{x_2+1}{2}\right)^{x_2+2}\left(\frac{x_1+1}{2}\right)^{x_1+2} \\[2mm] \cdot k^{2k+1} \\[2mm] \cdot e^{-(x_3+x_2+x_1+2k+3)} \\[2mm] \cdot e^{\frac{2}{12k+1}+\frac{2}{6(x_3+1)+1}+\frac{2}{6(x_2+1)+1}+\frac{2}{6(x_1+1)+1}} \end{array} \right)$$

After computations similar to those in previous cases, we see it suffices to show

$$e^2(x_3+1)(k-1)^{2k}e^{\frac{2}{3(k-1)}} \overset{!}{\leq} \frac{\sqrt{2\pi}}{8}k^{2k+1}\sqrt{(x_1+1)(x_2+1)(x_3+1)}.$$

As in Case 1(b), it suffices to show

$$e \overset{!}{\leq} \frac{\sqrt{2\pi}}{8}\sqrt{(x_1+1)(x_2+1)(x_3+1)}$$

with $x_1 + 1 \geq \frac{2k+4}{3}$, $x_2 + 1 \geq 2$, $x_3 + 1 \geq 2$. The desired inequality holds for

$$k \geq \frac{12e^2}{\pi} - 2 \approx 26.224$$

or all odd $k \geq 27$. $\qquad\square$

Our second special case concerns a certain family of CB graphs with an even number of vertices where the two cycles share exactly one edge.

Proposition 2.3.10. *Let $n = 2k \geq 10$.*

(i) If k is even,
$$N(CB(k, k, 1)) \leq M(2k).$$

(ii) If k is odd,
$$N(CB(k + 1, k - 1, 1)) \leq M(2k).$$

The proof uses the following observations, all of which follow from straightforward computations after expanding the right hand sides.
If k is even,
$$M(2k) = \left(\frac{k + 2}{2}\right)\left(\frac{k}{2}\right) F(k + 1, k - 1, 1). \tag{2.6}$$

If k is odd,
$$M(2k) = \left(\frac{k + 1}{2}\right)^2 F(k, k, 1). \tag{2.7}$$

For even k
$$M(2k - 2) = \frac{k}{2(k + 1)} M(2k - 1). \tag{2.8}$$

For odd k
$$M(2k - 2) = \frac{k - 1}{2k} M(2k - 1). \tag{2.9}$$

For all k
$$M(2k - 1) = \frac{1}{2} M(2k). \tag{2.10}$$

Finally, if k is even,
$$N(C_k) = \frac{4}{k} N(C_{k-1}) \tag{2.11}$$

Proof of Proposition 2.3.10. For even k, we have
$$\begin{aligned}
N(CB(k, k, 1)) &= N(C_k \vee C_k) + k^2 F(k - 1, k - 1, 1) \\
&\stackrel{(2.11),(2.7)}{=} \frac{16}{k^2} N(C_{k-1} \vee C_{k-1}) + \frac{4k^2}{k^2} M(2k - 2) \\
&\stackrel{\text{Def } 2.2.3}{=} \frac{16}{k^2} M(2k - 3) + 4M(2k - 2) \\
&\stackrel{(2.10),(2.8)}{=} \frac{2}{k(k + 1)} M(2k) + \frac{k - 1}{k} M(2k) \\
&= \frac{k^2 + 1}{k^2 + k} M(2k) \leq M(2k).
\end{aligned}$$

For odd k,

$$N(CB(k+1, k-1, 1)) = N(C_{k+1} \vee C_{k-1}) + k^2 F(k-1, k-1, 1)$$

$$\overset{(2.11),\,(2.6)}{=} \frac{16}{(k+1)(k-1)} N(C_k \vee C_{k-2}) + \frac{4(k+1)(k-1)}{(k+1)(k-1)} M(2k-2)$$

$$\overset{\text{Def } 2.2.3}{=} \frac{16}{(k+1)(k-1)} M(2k-3) + 4M(2k-2)$$

$$\overset{(2.10),(2.9)}{=} \frac{2}{k(k+1)} M(2k) + \frac{k}{k+1} M(2k)$$

$$= \frac{k^2+2}{k^2+k} M(2k) \leq M(2k).$$

$\square$

2.4 Further Conjectures and Open Problems

Through the course of this study, we observed several patterns that remain as conjectures and open questions. First, computational evidence suggests interesting structure for the function $F(x_1, x_2, x_3)$ beyond Theorem 2.3.8. We formally record our observations as the following conjecture, which has been confirmed with SageMath [29] for all n less than or equal to 399.

Conjecture 2.4.1. *For $n = 2k$ and $k \geq 2$ with $x_1 + x_2 + x_3 = n+1$, $F(x_1, x_2, x_3)$ is maximized at $F(n-1, 1, 1)$. For $n = 2k-1$ and $k \geq 3$ with $x_1 + x_2 + x_3 = n+1$, $F(x_1, x_2, x_3)$ is maximized at $F(n-3, 2, 2)$. Further, for any $x_1 \geq x_2 \geq x_3 \geq 3$ all even or all odd positive integers,*

$$F(x_1, x_2, x_3) \leq F(x_1 + 2, x_2, x_3 - 2)$$

and

$$F(x_1, x_2, x_3) \leq F(x_1 + 2, x_2 - 2, x_3),$$

when the subtraction by 2 will maintain the inequalities on the x_i's.

For example, the first inequality in Conjecture 2.4.1 asserts that for $x_1 \geq x_2 \geq x_3 \geq 5$ all of the same parity,

$$\sum_{j=0}^{x_3} \binom{x_3}{j} \binom{x_2}{\frac{1}{2}(x_2 - x_3) + j} \binom{x_1}{\frac{1}{2}(x_1 - x_3) + j}$$

$$\leq \sum_{j=0}^{x_3-2} \binom{x_3 - 2}{j} \binom{x_2}{\frac{1}{2}(x_2 - x_3 + 2) + j} \binom{x_1 + 2}{\frac{1}{2}(x_1 - x_3) + j}.$$

If proven, Conjecture 2.4.1, would strengthen Theorem 2.3.8. For a fixed n, not only would we know that any value of $F(x_1, x_2, x_3)$ was bounded above by $M(n)$, but also we would get a partial ordering on triples (x_1, x_2, x_3) satisfying the conditions of the conjecture that is induced by the inequalities on F.

Second, the remaining case for Conjecture 2.2.4 is the following.

Conjecture 2.4.2. *If x_1, x_2, and x_3 have different parities, then $N(CB(x_1, x_2, x_3)) \leq M(n)$.*

Using the recursion given by Corollary 2.3.6 part (ii) and the inequality $x_i \leq n$, it is straightforward to deduce that $N(CB(x_1, x_2, x_3)) \leq 6n^2 M(n)$. It is not clear to the authors how to obtain a stronger bound in this case. One direction toward proving Conjecture 2.4.2 is the following.

Conjecture 2.4.3. *For $n \geq 10$, $N(CB(x_1, x_2, x_3))$ with $x_1 + x_2 + x_3 = n + 1$ is maximized by*

$$\begin{cases} CB(k-1, k-1, 2) & n = 2k-1, k \text{ even} \\ CB(k, k-2, 2) & n = 2k-1, k \text{ odd} \\ CB(k, k, 1) & n = 2k, k \text{ even} \\ CB(k+1, k-1, 1) & n = 2k, k \text{ odd} \end{cases}.$$

Using SageMath [29], we have computed $N(CB(x_1, x_2, x_3))$ for all tuples with $x_1 + x_2 + x_3 = n + 1 \leq 535$. All of these values are less than or equal to the number of facets of our conjectured maximizer for the corresponding n, providing significant support for Conjecture 2.4.3.

Third, when n is even, Proposition 2.3.10 gives that the number of facets given by these conjectured maximizing graphs remains less than $M(n)$. Currently, for odd n we do not know of an equality or a bound strong enough to accomplish what Equations (2.6) and (2.7) give for even n. Therefore, a similar result for odd n remains unproven. We have verified that such a result holds for all odd n less than 100,000 via computations with SageMath [29].

Fourth, throughout our investigations we sought examples of graphs having a high number of symmetric edge polytope facets. Conjecture 2.0.2 asserts that graphs appearing as global facet-maximizers for connected graphs on n vertices can be constructed from minimally intersecting odd cycles, but it is unclear how to prove this. A related problem would be to prove that the graphs appearing as global facet maximizers in Conjecture 2.0.2 are facet maximizers among connected graphs having a fixed number of edges. We explore this idea a bit further in the special case of the following graphs, which are the conjectured global facet maximizers for connected graphs on an odd number of vertices.

Definition 2.4.4. Let $WM(n, r)$ denote the *windmill* graph on n vertices consisting of r copies of the cycle C_3 and $n - 1 - 2r$ edges all wedged at a single vertex. We say a windmill is *full* if n is odd and $r = \frac{n-1}{2}$. In other words, a full windmill is a wedge of $\frac{n-1}{2}$ triangles at a single vertex. Denote by $WM(n)$ the full windmill on n vertices.

Proposition 2.4.5. *For all odd n,*

$$N(WM(n)) = 6^{\frac{n-1}{2}}$$

$WM(7,2)$ $WM(8,2)$
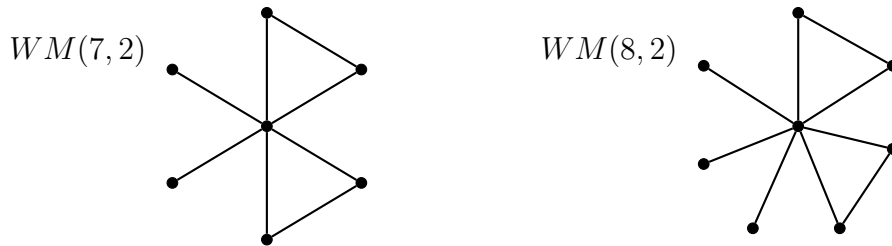
Figure 2.8: Two windmill graphs which are not full.
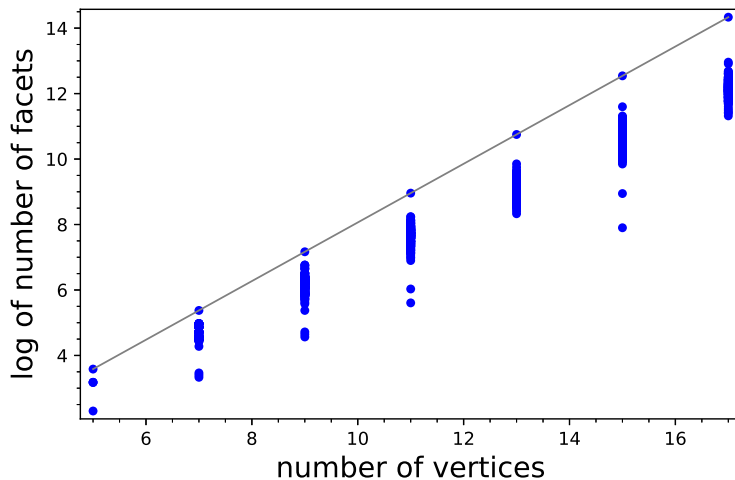
Figure 2.9: For each odd n between 5 and 17, the plot shows the log of the number of facets of P_G for samples of graphs G with n vertices and $3(n-1)/2$ edges with a target sample size of 200 graphs for each n. The line is $y = \frac{\log(6)}{2}(x-1)$, indicating $N(WM(n))$ for each n.

Proof. The windmill $WM(n)$ is a join of $\frac{n-1}{2}$ 3-cycles. By Lemma 2.1.5 and Proposition 2.1.4,

$$N(WM(n)) = (N(C_3))^{\frac{n-1}{2}} = 6^{\frac{n-1}{2}}.$$

$\square$

Conjecture 2.4.6. *Among graphs with n vertices and $3(n-1)/2$ edges (for odd n), WM(n) is a facet maximizer.*

To support this conjecture, we used SageMath [29] to sample the space of connected graphs with n vertices and $3(n-1)/2$ edges using a Markov Chain Monte Carlo (MCMC) technique similar to what is described in Section 2 of [12]. Then we computed $N(P_G)$ for each graph G in our sample. More detailed descriptions of this sampling process and its implementation are given in Section 3.2.

We generated sample families of graphs for all odd n between 5 and 17. The results of our sampling, shown in Figures 2.9 and 2.10, support Conjecture 2.4.6 for these values of n.
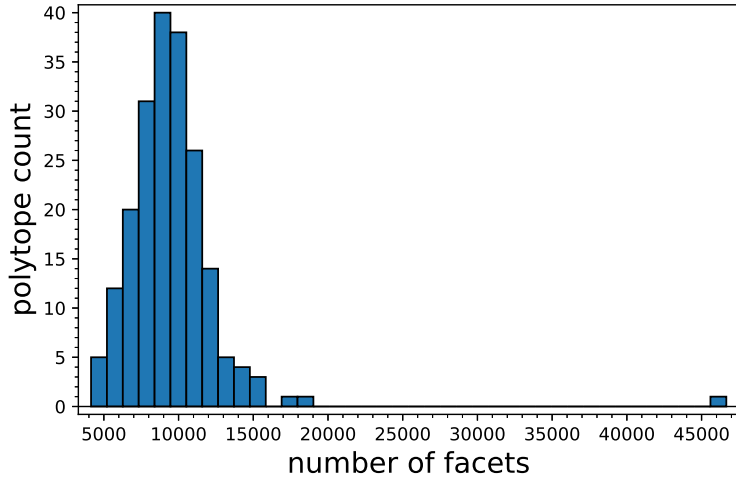
Figure 2.10: For $n = 13$, the histogram shows the distribution of $N(P_G)$ for our sample graphs. Not only does the maximum number of facets in our sample occur at $6^6 = N(WM(13))$, but there is a significant gap between our maximizer and all other facet counts in our sample.

Finally, it would be interesting to see if the framework of "facet-defining functions" for symmetric edge polytopes that was established by Higashitani, Jochemko, and Michałek in [15] could be applied to find a combinatorial description of faces of other dimensions. For example, given a symmetric edge polytope with dimension d, on could explore whether the functions that define two facets that intersect in a face of dimension $d - 2$ have a predictable relationship in terms of the graph. If something like this is possible, we would have a more complete picture of the face lattices for these polytopes.

Overall, the complexity of understanding facets and determining which graphs are facet-maximizers in a case as small as graphs with n vertices and $n + 1$ edges was unexpected. It indicates that there are many factors at play, and that other techniques and approaches may be necessary in the study of symmetric edge polytopes.

Chapter 3 Facets of Random Symmetric Edge Polytopes, Degree Sequences and Clustering

As evidenced in Chapter 2, understanding the facets of symmetric edge polytopes is not straightforward, even when the structure of the underlying graph is very restricted. Therefore, changing the perspective from which we viewed the structure of the graphs in the hope of gaining new insights became a task of interest. Our goal in the work presented in this chapter was to study the facet structure of P_G for various random graph models. The hope was that, through this investigation, we could determine what sorts of restrictions produce families of graphs for which we could possibly prove results in the future. This chapter is based on joint work with Benjamin Braun and Matthew Kahle. A pre-print is available here [3].

First, we investigate properties of the facets of P_G when G is an Erdős-Renyi random graph, establishing a threshold probability for which P_G and P_{K_n} share facet-supporting hyperplanes. Second, we present the results of empirical investigations regarding the relationship between clustering metrics on G and $N(G)$. The graph metric of interest in this work is the *average local clustering coefficient of G*, also called the *Watts-Strogatz clustering coefficient*. For each vertex v of G, define the local clustering coefficient $C_{WS}(v)$ to be the number of edges connecting two neighbors of v divided by the number of possible edges between neighbors of v. The average local clustering coefficient is then defined as

$$ C_{WS} = \frac{1}{|V(G)|} \sum_{v \in V(G)} C_{WS}(v) \, . $$

This value is a measure of graph transitivity introduced by Watts and Strogatz [31] in the context of network science.

Example 3.0.1. For any odd n, the full windmill $WM(n)$ has $C_{WS} = 1$. Any graph containing no cycles of length 3 has $C_{WS} = 0$.

Figure 3.1 contains a plot of average local clustering against number of facets for all $11,117$ connected graphs on 8 vertices. There are some apparent patterns in this data. For example, we have that $N(K_8) = 254$ and there are many graphs with $N(G) \approx 254$ having a wide range of clustering values. Further, there is a general trend that the number of facets increases with the clustering; the slope of the fit line for this data is approximately 148.46.

Given the rapid rate at which the number of connected graphs on n vertices grows, and the computational expense of computing the facets of a polytope given its vertices [27], it is not productive to attempt to compute facet data for all connected graphs on n vertices in general. However, in this paper we extend our observations for the $n = 8$ data by considering experimental evidence for various families of graphs with a fixed graph invariant. These experiments involve generating ensembles of graphs via well-known Markov Chain Monte Carlo techniques. Specifically,
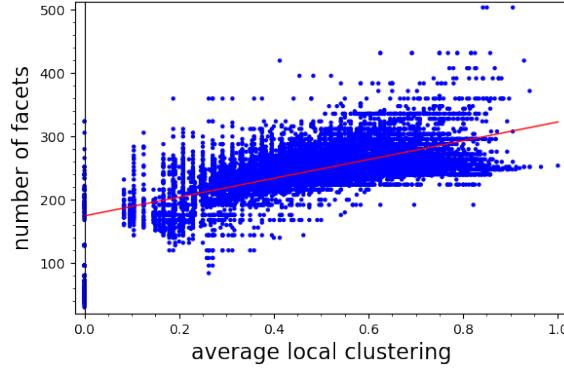
Figure 3.1: Average local clustering against number of facets for every connected graph G with 8 vertices. The line of best fit for this data is also included.

we present experimental evidence that for connected graphs with a fixed degree sequence, higher average local clustering tends to produce symmetric edge polytopes with a larger number of facets than those with lower clustering. All computations in this work were done with SageMath [29] (for graph generation/sampling and clustering metrics) and Normaliz [4, 5] (for facet computations). Because it is computationally expensive to compute the number of facets for a polytope, we limit our empirical studies to ensembles of graphs with less than 20 vertices; this corresponds to polytopes of dimension at most 19.

In this chapter, Section 3.1 contains an investigation of the number of facets for random graphs using the Erdős-Renyi model. We provide empirical data and we prove asymptotic results regarding the existence of certain facets for random graphs. In Section 3.2, we use Markov Chain Monte Carlo sampling techniques to generate random ensembles of graphs with either a fixed number of edges or a fixed degree sequence, and consider the relationship between average local clustering and facet numbers. Finally, in Section 3.3, we provide a toy example of a theoretical study regarding facet-maximizing graphs with a fixed degree sequence, and we conclude with a general discussion of our results and data.

3.1 The Erdős-Renyi Model

A standard model for empirically sampling graphs is the Erdős-Renyi model, denoted $G(n, p)$, for n a positive integer and $0 < p < 1$. In $G(n, p)$, each edge occurs independently with probability p. Thus, any fixed graph on n vertices having m edges occurs with probability $p^m (1-p)^{\binom{n}{2} - m}$, and the probability of a graph sampled from $G(n, p)$ having exactly m edges is $\binom{\binom{n}{2}}{m} p^m (1-p)^{\binom{n}{2} - m}$. Note that for $G = (V, E) \sim G(n, p)$, meaning a random graph sampled from $G(n, p)$, the expected value of C_{WS} is p.

3.1.1 Facets of $G(n,p)$

There are many well-known limitations to the model $G(n,p)$, most notably that the expected degree distribution, average shortest path length, and various clustering metrics often do not match observations in real-world networks [21]. However, one of the major advantages of working with $G(n,p)$ is that it is defined in a way that often allows theoretical results to be obtained. For example, see [10] for the use of the $G(n,p)$ model in the study of Ehrhart theory for symmetric edge polytopes. In this subsection, we prove that for certain values of p, the typical $G(n,p)$ will have facets of a prescribed form. To do this, we again make use of Theorem 2.1.1 and Lemma 2.1.2, which were discussed in Section 2.1. Here we study the expected structure of induced bipartite subgraphs of $G(n,p)$ across various bipartitions of the vertex set, as these are the candidates for facet subgraphs.

Definition 3.1.1. For any bipartition $(A, V \setminus A)$ of the vertex set V of a graph G, we denote by $B(A, G)$ the induced bipartite subgraph for the bipartition $(A, V \setminus A)$.

Note that given any bipartition $(A, V \setminus A)$ of the vertex set of G, if $B(A, G)$ is connected then there are at least two facets of P_G having $G_f = B(A, G)$, specifically the two $\{0, 1\}$-labelings of the shores of the bipartition. When $G = K_n$, any bipartition produces a facet subgraph and these $\{0, 1\}$-labelings are the only facet-supporting functions.

Thus, we are interested in understanding when $B(A, G)$ is connected for an typical G. For the following theorem, recall that a sequence of events $\mathcal{A}_n$ for $n = 1, 2, \ldots$ occurs *with high probability* (abbreviated w.h.p.) if $\lim_{n \to \infty} Prob(\mathcal{A}_n) = 1$.

Theorem 3.1.2. *Let $G = (V, E) \sim G(n, p)$.*

- *If $p < 1/2$ is fixed, then w.h.p. there exists an $\lfloor n/2 \rfloor$-subset A of V such that $B(A, G)$ is not connected.*

- *If $p > 1/2$ is fixed, then w.h.p. for every subset $A \subset V$, $B(A, G)$ consists of a single connected component unioned with isolated vertices.*

- *Further, if $p = 1/2 + \epsilon$ is fixed, then w.h.p. for every subset $A \subset V$ with $||A| - n/2| < \epsilon(1/2 - \epsilon)n$ we have that $B(A, G)$ is connected and spans V.*

The proof of Theorem 3.1.2 will require the following well-known lemma.

Lemma 3.1.3. *Let $p \in (0, 1)$ be fixed, and $G \sim G(n, p)$. Then w.h.p. every vertex in G has degree $\approx pn$. That is, for every fixed $\epsilon > 0$, w.h.p. every vertex v has degree $(1 - \epsilon)pn < deg(v) < (1 + \epsilon)pn$.*

Using this lemma, we'll prove Theorem 3.1.2 by showing that w.h.p. an induced bipariitite subgraph of $G \sim G(n, p)$ does have a component of a certain size when $p < 1/2$ and does not have any components of certain sizes when $p > 1/2$. At this time, we have not explored what occurs when $p = 1/2$.

Proof of Theorem 3.1.2. For the case where $p < 1/2$, note that w.h.p. every vertex has degree close to its mean pn. Since $p < 1/2$, a typical vertex v is connected to fewer than half of the other vertices. Thus, there is some $\lfloor n/2 \rfloor$-subset A of V containing the entire neighborhood of v, and the corresponding $B(A, G)$ is not connected.

Next, let $p = 1/2 + \epsilon$ for fixed $\epsilon > 0$. First, we show that for any subset $A \subset V$, there exists a constant $\alpha \in \mathbb{R}_{>0}$ depending only on ϵ such that $B(A, G)$ has no connected component of order i for $2 \le i \le \lfloor \alpha n \rfloor$. Let $\delta = \delta(G)$ denote the minimum degree of a vertex in G. By Lemma 3.1.3, w.h.p. $\delta \ge (1-\epsilon)(1/2+\epsilon)n = \dfrac{(1 + \epsilon)}{2}n - \epsilon^2 n$. For the bipartition $(A, V \setminus A)$, one of A and $V \setminus A$ has order less than or equal to $n/2$. Without loss of generality, suppose $|A| \le n/2$. If $S \subset V$ spans a connected component of $B(A, G)$ and $|S| \ge 2$, then there exists a vertex v of S such that $v \in A$. Then w.h.p. $\deg(v) \ge \frac{(1+\epsilon)}{2}n - \epsilon^2 n$ and the number of neighbors of v that are in $V \setminus A$ must be at least

$$\delta - |A| \ge \frac{(1 + \epsilon)}{2}n - \epsilon^2 n - n/2$$
$$= \frac{\epsilon n}{2} - \epsilon^2 n$$
$$= \epsilon(1/2 - \epsilon)n.$$

Setting $\alpha = \frac{\epsilon}{2}(1/2 - \epsilon)$, we see that w.h.p. the order of S is strictly greater than αn, a contradiction.

Next we rule out connected components of order i for $\lceil \alpha n \rceil \le i \le \lfloor 2n/3 \rfloor$. We do this by bounding the probability that a given subset of i vertices spans a connected component for some bipartition $(A, V \setminus A)$. Suppose toward a contradiction that $S \subset V$ with $|S| = i$ spans a connected component of $B(A, G)$, and let $a = |S \cap A|$ and $b = |S \cap (V \setminus A)|$. Any edge between $S \cap A$ and $(V \setminus A) \setminus S$ is forbidden. If there was such an edge, S would not span its connected component, contradicting our assumption. The same holds for edges between $A \setminus S$ and $S \cap (V \setminus A)$. So the number of forbidden edges is $a(n - b) + b(n - a) = (a + b)n - 2ab$, and the probability that S spans its component in the given bipartition is at most

$$(1 - p)^{(a+b)n - 2ab}.$$

Since $a + b = i$, ab is maximized when $a = \lfloor i/2 \rfloor$ and $b = \lceil i/2 \rceil$. Thus, the number of forbidden edges is at least

$$in - 2(i/2)^2 = i(n - i/2) \ge (\alpha n)(n - n/3) = \frac{2\alpha}{3}n^2.$$

So the probability that a fixed subset S spans a connected component for a fixed bipartition $(A, V \setminus A)$ is bounded above by

$$(1 - p)^{\frac{2\alpha}{3}n^2}.$$

38

Applying a union bound, the probability that there exists an i-element subset that spans a connected component for a fixed bipartition is bounded above by

$$\sum_{i=\lceil \alpha n \rceil}^{\lfloor 2n/3 \rfloor} \binom{n}{i}(1-p)^{\frac{2\alpha}{3}n^2}.$$

Applying a union bound again to consider all bipartitions, the probability that there is any connected component of size $\lceil \alpha n \rceil \leq i \leq \lfloor \frac{2n}{3} \rfloor$ in any bipartition is bounded above by

$$\sum_{k=1}^{n-1} \binom{n}{k} \sum_{i=\lceil \alpha n \rceil}^{\lfloor 2n/3 \rfloor} \binom{n}{i}(1-p)^{\frac{2\alpha}{3}n^2} \leq 2^n \cdot 2^n (1-p)^{\frac{2\alpha}{3}n^2} \to 0$$

as $n \to \infty$ since $p \in (0,1)$ is fixed. So w.h.p. $B(A,G)$ consists of a single large component of order at least $2n/3$ unioned with isolated vertices.

Now we show that if $||A|-n/2| < \epsilon(1/2-\epsilon)n$, then w.h.p. $B(A,G)$ has no isolated vertices. We know that for $p = 1/2 + \epsilon$ we have $\delta \geq \frac{(1+\epsilon)}{2}n - \epsilon^2 n$. For a bipartition $(A, V \setminus A)$, one of the shores has size greater than $n/2$; we have already seen that if $|A| < n/2$, w.h.p. there are no isolated vertices in $B(A,G)$ contained in A (they each have a neighbor in $V \setminus A$). Thus, we can assume that $|A| > n/2$ and assume further that $|A| - n/2 < \epsilon(1/2 - \epsilon)n$. It follows that

$$|A| < \frac{(1+\epsilon)}{2}n - \epsilon^2 n = \delta$$

and thus $\delta - |A| > 0$. Hence, w.h.p. every vertex in A must have a neighbor in $V \setminus A$ and thus there are no isolated vertices in $B(A,G)$. $\square$

Theorem 3.1.2 establishes a large family of facet subgraphs G_f for $G \sim G(n,p)$ that exist with high probability when $p > 1/2$. Observe that every facet subgraph must support the two facet-defining functions taking values in $\{0,1\}$, namely those two 0/1-functions that are constant on the shores of the bipartition induced by G_f. Further, note that any 0/1-function on the vertices of G is a facet-defining function for the symmetric edge polytope of the complete graph on those vertices because every bipartition of the vertices of a complete graph induces a connected bipartite subgraph. Thus, Theorem 3.1.2 shows that when $p > 1/2$ and n is large, there are many symmetric pairs of facet-supporting hyperplanes that are identical for $G \sim G(n,p)$ and K_n. The corresponding facets might not have the same polyhedral structure in the two symmetric edge polytopes, but the facet-supporting hyperplanes are the same. This leads to the following corollary.

Corollary 3.1.4. *Let $G = (V,E) \sim G(n,p)$. For fixed $p = 1/2 + \epsilon$, let $t(n,p)$ denote the number of subsets $A \subset V$ satisfying $||A| - n/2| < \epsilon(1/2-\epsilon)n$. Then w.h.p. we have that the number of facets of P_G is at least $t(n,p)$.*

Example 3.1.5. Figure 3.2 shows two graphs, a path with 3 vertices and a complete graph with 3 vertices, and their symmetric edge polytopes. The bold pairs of facets are supported by the same pair of hyperplanes, in particular, the hyperplanes $x_v = 1$ and $x_u + x_w = 1$, arising from the partition $(\{u, w\}, \{v\})$ of the vertices. Since the path graph does not contain the edge uw, it is not necessary that the facet-defining functions be constant on the shores of this partition. Therefore, this same partition also determines the other pair of facets for the path graph, supported by the hyperplanes $x_u - x_w = 1$ and $x_w - x_u = 1$, which are not support hyperplanes for K_3.
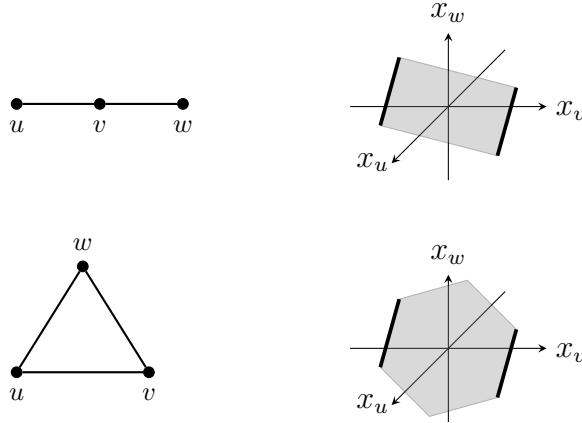

Figure 3.2: A path graph P_3 (top) and the complete graph K_3 (bottom) with their symmetric edge polytopes. Facets arising from the same pair of support hyperplanes are bold.

The next corollary shows that with high probability, there is at least one G_f in $G \sim G(n, 1/2 + \epsilon)$ that supports for P_G only the facet-supporting hyperplanes that the same bipartition supports for P_{K_n}.

Corollary 3.1.6. *Let $G_n = (V_n, E) \sim G(n, p)$. If $p = 1/2 + \epsilon$ is fixed, then for a sequence of subsets $A_n \subset V_n$ with $||A_n| - n/2| < \epsilon(1/2 - \epsilon)n$, w.h.p. there are only two facet functions f of P_{G_n} with $G_f = B(A_n, G)$, namely the functions f with values in $\{0, 1\}$.*

Proof. First note that as $n \to \infty$, w.h.p. the induced subgraph of G on a given subset of vertices A with $|A| > ((1+\epsilon)/2 - \epsilon^2)n$ is connected. To see this, note that since ϵ is fixed, we have $((1+\epsilon)/2 - \epsilon^2)n$ goes to infinity and thus $p = 1/2 + \epsilon > \log(((1+\epsilon)/2 - \epsilon^2)n)/((1+\epsilon)/2 - \epsilon^2)n$. Thus, the induced subgraph is $G(((1+\epsilon)/2 - \epsilon^2)n, p)$ and, by a well-known theorem of Erdős and Renyi, w.h.p. this is connected. Since both $B(A, G)$ and $B(V \setminus A, G)$ are connected w.h.p. for any A with $||A| - n/2| < \epsilon(1/2 - \epsilon)n$, it follows from Theorem 2.1.1 that any f with $G_f = B(A, G)$ is constant on both A and $V \setminus A$. $\qquad \square$

Example 3.1.7. The graph G in Figure 3.3 is the subgraph of the complete graph K_4 obtained by removing the edge vw. The bipartition $(\{t, v\}, \{u, w\})$ of the vertices

of G produces the facet subgraph G_f. Since the edges tv and uw are present in the original graph G, Theorem 2.1.1 gives that any facet-defining function must be constant on the shores of this bipartition. In particular, the only facet-supporting hyperplanes of P_G that arise from this partition are $x_t + x_v = 1$ and $x_u + x_w = 1$, which are exactly the facet-supporting hyperplanes for P_{K_4} associated with the same partition.
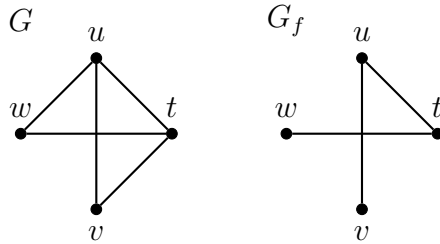
Figure 3.3: The graph G is formed by removing the edge vw from the complete graph K_4. The graph G_f is the facet subgraph of G associated to the partition $(\{t, v\}, \{u, w\})$ of the vertices.

3.1.2   Data and Observations

While Theorem 3.1.2 establishes the existence of many facet subgraphs in certain large random graphs, this does not provide much insight into our consideration of average local clustering. When we direct our attention to empirical data for $G(n, p)$, no apparent correlation between average local clustering and $N(G)$ is observed, as demonstrated in Figure 3.4 for an ensemble sampled from $G(14, 0.45)$. This is in stark contrast to the data for all connected graphs on eight vertices shown in Figure 3.1. One caveat is that there are $29{,}003{,}487{,}462{,}848{,}061$ connected graphs on 14 vertices [17, A001349], of which we sample only 4975. Figure 3.5 provides further evidence that sampling from $G(n, p)$ does not yield a consistent trend. This figure contains a table of plots providing data for ensembles of graphs with $n = 11, 14, 17$ and $p = 0.2, 0.4, 0.6, 0.8$.

Figure 3.4: Data from an ensemble of 4975 connected graphs from $G(14, 0.45)$.

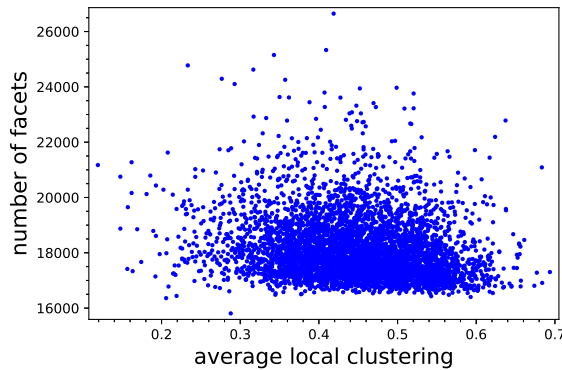In Figure 3.5, the number of vertices increases across rows while the value of p increases down columns. As expected, the mean value of sampled C_{WS} values is approximately p. Further, reading down each column as p increases, we observe the range of values of $N(G)$ in our sample becomes smaller. Specifically, these values are getting closer to $N(K_n) = 2^n - 2$, where this formula is a straightforward application of Theorem 2.1.1. This makes sense, as higher values of p leads to greater edge density, and thus the typical sampled graph is closer in structure to K_n.

What we do not see consistently in these samples from $G(n, p)$ is a positive correlation between average local clustering and number of facets that is observed in Figure 3.1. In fact, some samples exhibited a negative correlation. For $p = 0.2$, the first row in Figure 3.5, we do observe a positive trend. We also observe that when $p = 0.2$, there is significantly more variation in the number of facets that arise; note that for $n = 17$, the range of the vertical axis when $p = 0.2$ is from less than $100,000$ to over $400,000$. However, for $n = 17$ and $p = 0.8$, the range is from around $131,000$ to around $131,400$. Note that $N(K_{17}) = 131,070$.

What we will see in Section 3.2 is that when we sample graphs on n vertices in a more restrictive fashion, fixing also the number of edges or (more strongly) the degree sequence, we do observe a positive correlation between average local clustering and number of facets.

3.2 Graph Ensembles via Markov Chain Monte Carlo Sampling

While our samples from $G(n, p)$ for fixed p do not display the relationship between average local clustering and $N(G)$ that was observed in the complete enumeration for small n (as in Figure 3.1), we do see correlations when we use other random graph models that differently restrict the space of graphs we consider. This portion of our study uses Markov Chain Monte Carlo (MCMC) techniques to generate ensembles of connected graphs having either a fixed number of edges or a fixed degree sequence. These techniques arise in the study of configuration models for random graphs with a fixed degree sequence, see the survey [12] and the references given there for more details.

3.2.1 MCMC Sampling Methods

Sampling from graph spaces via Markov chain traversal is a common technique [12]. For a Markov chain having a certain stationary distribution, sample graphs taken at sufficiently spaced intervals can be treated as independent, and an ensemble of such graphs can be expected to follow the stationary distribution. In the case of our study, we employ Markov chains for which the stationary distribution is uniform arising from processes to produce new graphs from old by local, reversible operations. With this, we can picture the sample space as a graph of graphs $\mathcal{G}$, where each node represents a graph in the space, and there is a directed edge from the graph G to the graph G' if performing an instance of the transition operation on G produces G'. In general, each edge has a weight signifying the probability of that transition. In our study, all instances of the transition operation are equally likely. That is, from a
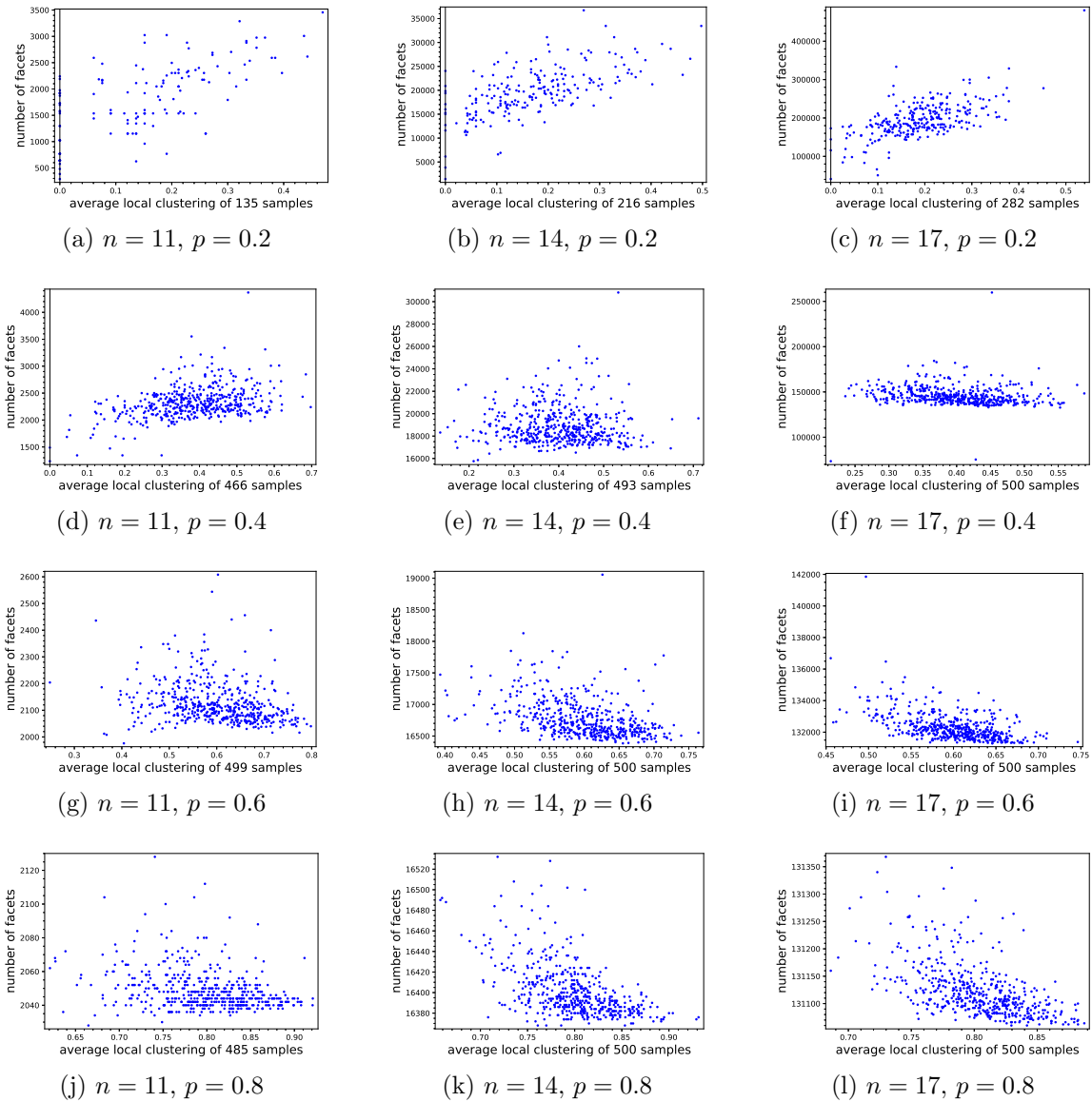
Figure 3.5: Data from ensembles drawn from $G(n, p)$. The target sample size in each ensemble was 500 connected graphs and disconnected graphs were rejected during sampling. Note that for smaller values of p, the range of the vertical axis is significantly larger than for large values of p.

state, G, in the Markov chain, the probability of transitioning to any adjacent state is equal. So we can view edges in the graph of graphs for our spaces as unweighted.

Fixed Number of Edges

To sample from the space of connected graphs with n vertices and m edges, we employ a single-edge replacement MCMC technique similar to what is described in [12, Section 2] (in the case of trees, this technique is known as branch exchange). Define

the graph of graphs $\mathcal{G}(n, m)$ to be the directed graph with vertex set all connected graphs with n vertices and m edges. A connected graph G has an arrow in $\mathcal{G}(n, m)$ to a connected graph G' if G' is obtained from G by deleting an edge in G and adding an edge in G' from the complement of G. This process is demonstrated in Figure 3.6.

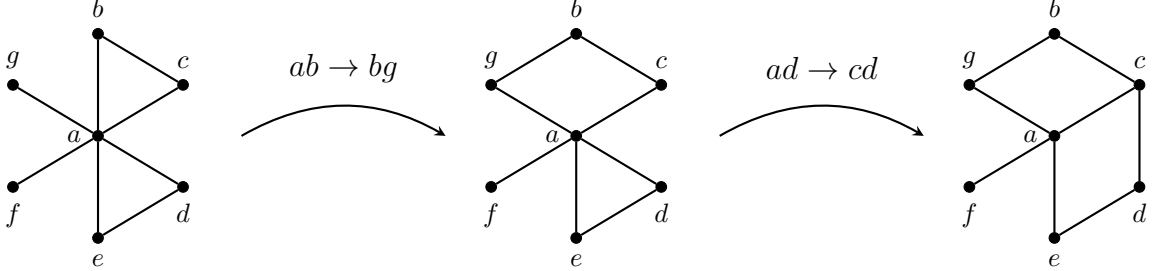Figure 3.6: An example of a walk through $\mathcal{G}(7, 8)$ demonstrating a sequence of two possible single-edge replacements, first replacing ab with bg, then replacing ad with cd.

Thus, note that every arrow in $\mathcal{G}(n, m)$ is reversible. Further, for an edge $e \in G$ and f in the complement of G, if the edge set $(E(G) \setminus \{e\}) \cup \{f\}$ does not form a connected graph, define $\mathcal{G}(n, m)$ to have a loop at G. It is straightforward to show that the directed graph $\mathcal{G}(n, m)$ is regular, strongly connected, and aperiodic, hence we can conclude that ensembles generated by this method asymptotically obey a uniform distribution [12]. Further details of the implementation of our sampling method are given in Subsection 4.2.2.

Fixed Degree Sequence

To sample from the space of simple connected graphs on n vertices with a fixed degree sequence, we employ a double-edge swap MCMC technique as described in [12, Section 2]. Define the graph of graphs $\mathcal{G}(\mathbf{d})$ to be the directed graph with vertex set all connected graphs with degree sequence $\mathbf{d}$. A connected graph G has an arrow to G' in $\mathcal{G}(\mathbf{d})$ if G' is obtained from G via a double-edge swap, i.e., if there exist edges uv and xy in G such that replacing these edges with ux and vy produces G'. An example is shown in Figure 3.7.

If performing a particular double-edge swap on G would produce a graph that is outside the space (i.e. the new graph has a loop or multiedge or is disconnected), that swap will correspond to a loop on the vertex G in $\mathcal{G}(\mathbf{d})$. It is shown in [12] that $\mathcal{G}(\mathbf{d})$ is regular, strongly connected, and aperiodic. Thus, as before, the samples asymptotically obey a uniform distribution. Further details of the implementation of our sampling method are given in Subsection 4.2.2.

3.2.2 Data and Observations

In each of our experiments, we generated an ensemble of graphs with specified invariants: number of vertices and either number of edges or degree sequence. For each of our samples, we computed the average local clustering and the number of facets
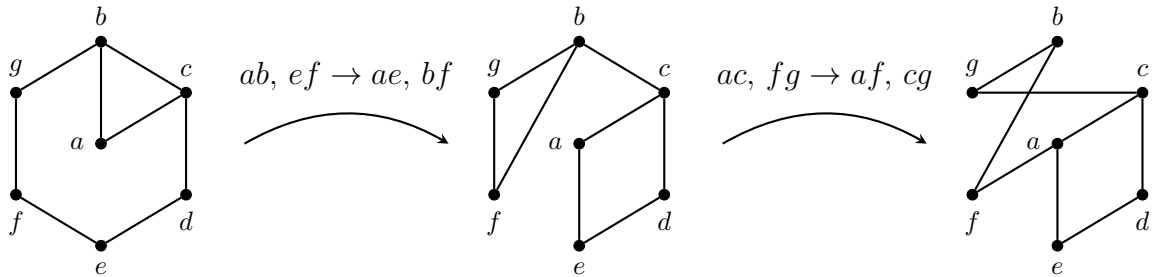
Figure 3.7: An example of a walk through $\mathcal{G}(\{3, 3, 2, 2, 2, 2, 2\})$ demonstrating a sequence of two possible double edge swaps, first swapping the endpoints of ab and ef, then swapping the endpoints of ac and fg.

for P_G, and we generated a plot displaying the results. We discuss these experiments and results in this subsection.

Fixed Number of Edges

We first used single-edge replacement MCMC methods to generate ensembles of graphs with a fixed number of vertices and edges. We computed $C_{WS}(G)$ and $N(P_G)$ for each graph in our ensemble, and plotted the resulting ordered pairs. In each of these plots, the number of facets appears to generally increase as C_{WS} increases. Additionally, we observe that these plots often exhibit heteroscedasticity, i.e., the variance of the data changes as C_{WS} increases. Figure 3.8 shows two representatives of the types of plots we observe.

(a) 1001 graphs with 11 vertices and 25 edges. (b) 201 connected graphs with 15 vertices and 37 edges
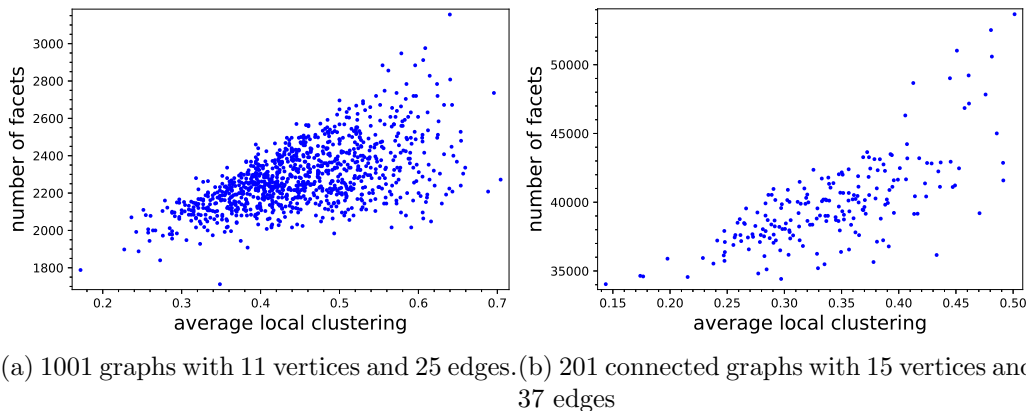
Figure 3.8: Fixed edge data for 11 and 15 vertices

Figure 3.9 contains plots for connected graphs on 11 vertices with various fixed numbers of edges. These plots suggest that the heteroscedasticity phenomenon, where the variance in the number of facets increases as average local clustering increases, arises across multiple fixed edge counts. It is important to note that in the data plots for Figure 3.9, all the axes change scale. Thus, for example, the plot for 11 vertices and 20 edges has average local clustering range from near 0 to 0.8, and facet

numbers range from under 2000 to over 4000. However, the plot with 35 edges has a significantly restricted range for both the horizontal and vertical axis. This is the same phenomenon that appeared in Figure 3.5, where higher edge density yields less variation for both average local clustering and facet numbers. Nevertheless, even at different scales, a positive correlation is observed.

(a) 11 vertices, 20 edges

(b) 11 vertices, 25 edges

(c) 11 vertices, 30 edges

(d) 11 vertices, 35 edges
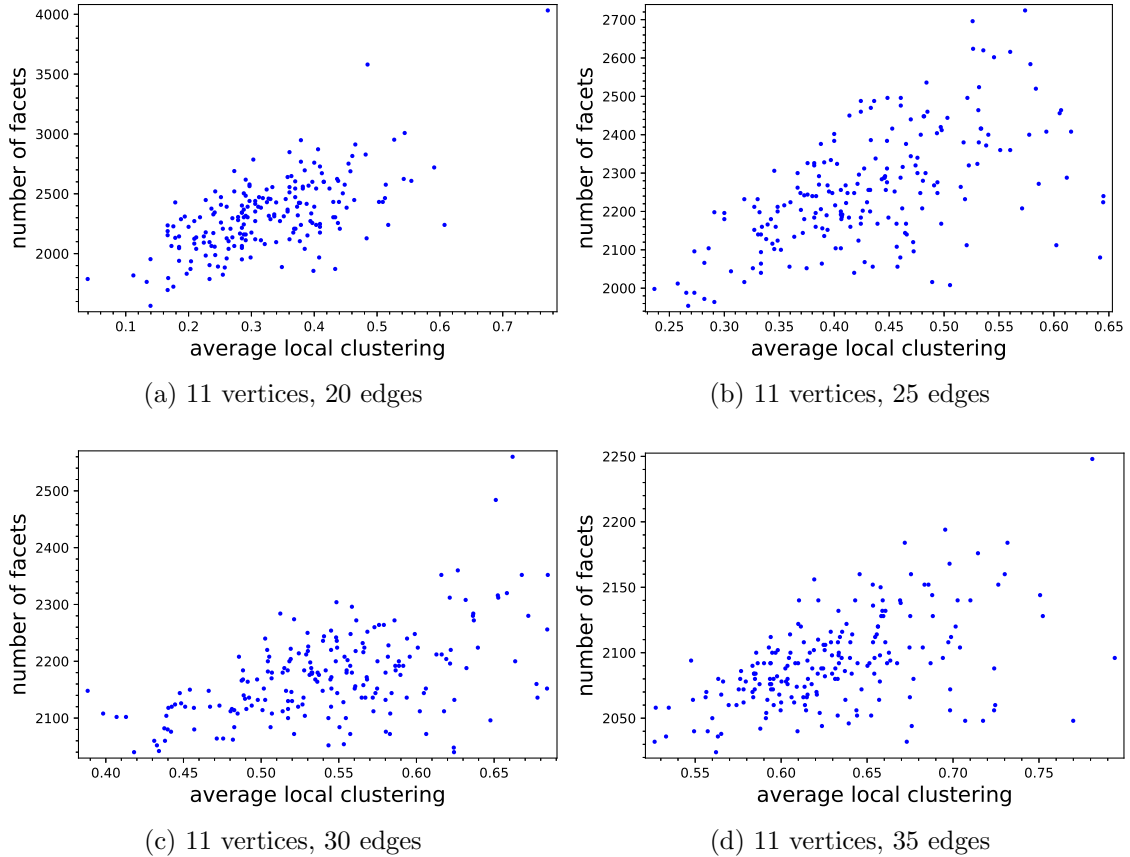
Figure 3.9: Data for graphs on 11 vertices with varying edge numbers

Graphs with Hubs

Our next experiments used double-edge swap MCMC methods to generate connected graphs with a fixed degree sequence. In real-world graphs, it is common for there to be a large number of lower-degree vertices and a small number of higher-degree vertices; the latter are often referred to as *hubs*. This has led to the development of various random graph models that exhibit scale-free degree distributions [21]. Because we are limited in the dimensions of P_G for which we can effectively compute the number of facets, the magnitude of hubs that we can study are not as great as often found in large real-world networks. However, Figures 3.10 and 3.11 are representative of the data we have observed in ensembles of graphs on less than 20 vertices where the degree sequence has a small number of high-degree vertices. In all of the experiments

we have conducted for graphs with hubs, a correlation between C_{WS} and $N(G)$ is observed.

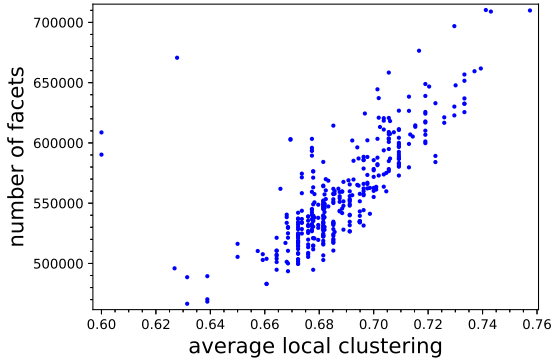Figure 3.10: Data from an ensemble of 370 connected graphs having 18 vertices and degree sequence $[3, 3, 4, 4, \ldots, 4, 4, 5, 5, 16, 16]$ obtained by MCMC with double-edge swaps.
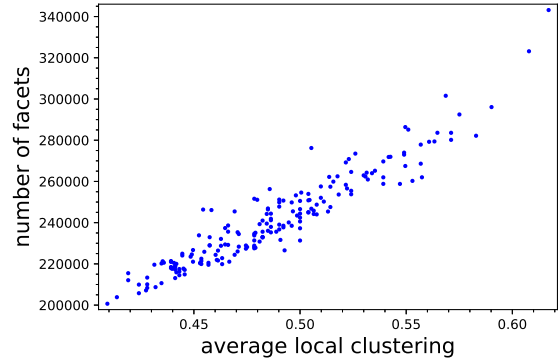
Figure 3.11: Data from an ensemble of 192 connected graphs with 17 vertices and degree sequence $[3, 3, 3, 4, \ldots, 4, 5, 5, 5, 5, 15]$ obtained by MCMC with double-edge swaps.

k-Regular Graphs

A classic family of graphs with a fixed degree sequence are k-regular graphs, i.e., graphs where every vertex has degree k. The number of connected regular graphs on n vertices is a well-studied integer sequence [17, A005177]. Based on our previous observations, for larger values of k the average local clustering should be higher, due to higher edge density. What is less clear is what to expect from the number of facets of the symmetric edge polytope as k varies, especially for small k.

Figure 3.12 provides a plot of average local clustering and number of facets for 3390 connected regular graphs on 12 vertices (that there are 18979 such graphs), sampled using double-edge MCMC for each k. Note that for small values of k, there is a trend that $N(G)$ increases as C_{WS} increases. When k is small, the average local clustering is generally less than 0.4 and the number of facets varies widely. As k increases, the average local clustering varies less, and the number of facets concentrates near the value of $N(K_{12}) = 4094$. In general, it is reasonable to expect that as the edge density of a k-regular graph G increases, and thus as the graph becomes closer to a complete graph, there will be many connected spanning bipartite subgraphs where the induced subgraph of G on each shore of the bipartition is connected.

Additional data plots from ensembles of k-regular graphs on 18 vertices for $k = 3, 7$ are given in Figures 3.13 and 3.14. Both of these plots further illustrate the phenomenon shown in Figure 3.12, where k-regular graphs for smaller k have significantly larger variance in the number of facets (as seen in the range of the vertical axes), and have lower average local clustering.
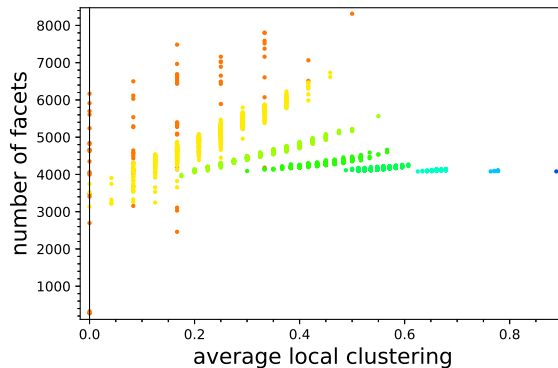
Figure 3.12: Data from a sample of 3390 connected k-regular graphs on 12 vertices obtained by MCMC with double-edge swaps, for $k = 3, 4, 5, 6, 7, 8, 9, 10$. Each value of k corresponds to a different color in the plot, with lower k having smaller C_{WS} values. Note that for larger k, the number of facets is approximately $N(K_{12})$.
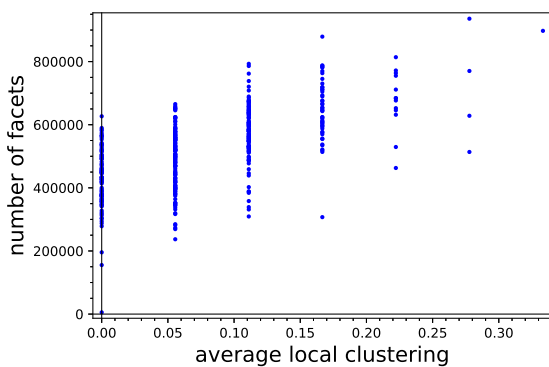
Figure 3.13: Data from an ensemble of 397 connected 3-regular graphs on 18 vertices obtained by MCMC using double-edge swaps. Note the large range of the vertical axis.
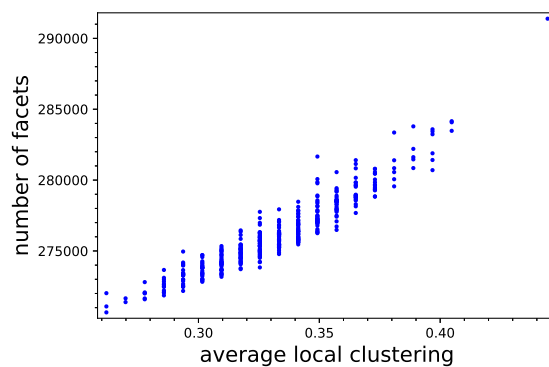
Figure 3.14: Data from an ensemble of 399 connected 7-regular graphs on 18 vertices obtained by MCMC using double-edge swaps. Note the narrow range on the vertical axis.

3.3 Discussion

It is extremely challenging to understand the facet structure of P_G for a random graph generated by any of the models we have considered in this work. We will discuss an example of a toy theoretical result in this direction prior to our final discussion.

3.3.1 Case: n Vertices, n Edges, Fixed Degree Sequence

When the number of vertices is equal to the number of edges, we can compute $N(P_G)$ for any connected graph with a fixed degree sequence. Further, we can describe a graph with that degree sequence that attains the maximum number of facets. This is possible because, in this case, $N(P_G)$ depends only on the length of the unique cycle in G. To get this facet information for a given degree sequence, we need only know

what lengths of cycle are attainable with that sequence.

Proposition 3.3.1. *Let G be a simple graph with n vertices and n edges with degree sequence $\mathbf{d} = \{d_i\}_{i=1}^n$ ($d_i \geq d_{i+1}$). Let m_G denote the minimum possible length of a cycle in G, and let M_G denote the maximum possible length of a cycle in G.*

(i) If $d_i = 2$ for all i, $m_G = M_G = n$.

(ii) If $d_k \geq 2$ and $d_i = 1$ for $i > k$ with $k < n$, $m_G = 3$ and $M_G = k$.

Proof. To show (i), note that the only simple connected graph with this degree sequence is the n cycle. So $m_G = M_G = n$.

To show (ii), we construct a simple, connected graph G with a cycle of length m for $3 \leq m \leq k$ with the following procedure.

1. Construct a cycle, C, on vertices $1, \ldots, m$.

2. If $m = k$, skip to (4). Otherwise, construct a path, P, on vertices $m + 1, \ldots, k$ with $k - (m + 1) \geq 0$ edges.

3. Now, $d_1 \geq 3$ and $d_{m+1} \geq 2$, so vertex 1 is incident to at least one edge not on C and vertex $m + 1$ is incident to at least one edge not on P. So we connect 1 and $m + 1$.

4. The remaining edges are incident to leaves. There are $n - k$ leaves and

$$n - (\text{number of edges of } C) - (\text{number of edges of } P) - 1$$
$$= n - m - (k - m - 1) - 1$$
$$= n - k$$

   edges that must be added. So there are exactly enough open half-edges on the vertices $1, \ldots, k$ to be filled by the leaves.

$\square$

Example 3.3.2. Consider the degree sequence $\{3, 3, 2, 2, 1, 1\}$ for a graph on 6 vertices with 6 edges. Following the steps in Proposition 3.3.1, we construct a graph with this degree sequence containing a 3-cycle ($m = 3$) as follows. An illustration of this construction is given in Figure 3.15.

1. Construct the 3-cycle C on the vertices $1, 2, 3$ each of which have degree at least 2. The vertex 3 now has the desired degree.

2. Since $m = 3 < 4 = k$, we construct the path P containing only the vertex 4 (a path with one vertex and no edges).

3. Since the degree of vertex 1 is 3, and it is incident to only two edges on C, we can add an edge between vertices 1 and 4 to connect the cycle to the path. The vertex 1 now has the desired degree.
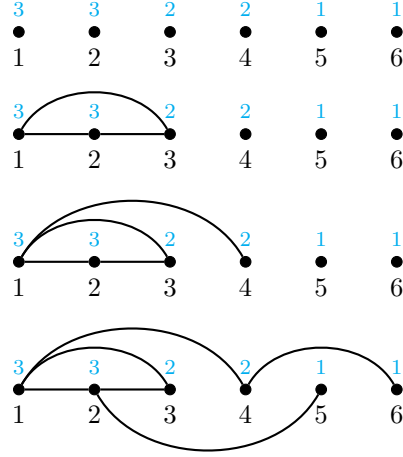
Figure 3.15: Construction of a graph with degree sequence $\{3, 3, 2, 2, 1, 1\}$ containing a 3-cycle via the algorithm in Proposition 3.3.1. The degree of each vertex is given in blue above the vertex.

4. Now, we must add one edge incident to each of the vertices 2 and 4. We have exactly enough leaves to add these necessary edges. Adding the edges $\{2, 5\}$ and $\{4, 6\}$ gives the desired degree for vertices 2, 4, 5, and 6.

Given Proposition 3.3.1, we can apply [2, Theorem 3.2] to a class of graphs with n vertices and n edges that have a specific degree sequence to identify the facet-maximizing graphs for that degree sequence. As in [2], we use the notation $G \vee H$ to denote a graph obtained by identifying graphs G and H at a single vertex.

Corollary 3.3.3. *Let G be a simple graph with n vertices and n edges with degree sequence $\{d_i\}_{i=1}^n$ ($d_i \geq d_{i+1}$). Let $N(G)$ denote the number of facets of the symmetric edge polytope P_G.*

(i) If $d_n = 2$,

$$N(G) = N(C_n).$$

(ii) If $d_k > 1$ and $d_{k+1} = 1$ for some $k < n$, and ℓ is the largest odd number satisfying $\ell \leq k$,

$$N(G) \leq N(C_\ell \vee P_{n-\ell})$$

Here, C_m denotes a cycle with m edges, and P_m denotes a path with m edges.

Even further than this, the proof of [2, Theorem 3.2] describes how $N(G)$ changes as the cycle length varies. For any degree sequence that allows a cycle of length at least 5, a graph G that maximizes $N(G)$ has $C_{WS}(G) = 0$. In fact, the only graphs on n vertices and n edges that have nonzero average local clustering are those that have a single 3-cycle. Even these graphs have C_{WS} approaching 0 as n increases.

50

A precise theoretical result was attainable in this case because the small number of edges relative to number of vertices significantly restricts the structure of the graphs we consider.

3.3.2   Final Discussion

The goal of this branch of investigation of symmetric edge polytopes was to study relationships between graph structure and facet structure, with a focus on both theoretical and empirical results for various random graph models. For Erdös-Renyi random graphs $G \sim G(n,p)$, we observed empirically that as p increases, the number of facets of P_G tends toward $2^n - 2$, the number of facets of P_{K_n}. We also established a threshold of $p > 1/2$ such that, with high probability, any sufficiently even bipartition $(A, V \setminus A)$ (i.e. having $||A| - n/2| < \epsilon(1/2 - \epsilon)n$) of the vertices of $G \sim G(n,p)$ induces a facet subgraph of G. Thus, with high probability, the number of such bipartitions gives a lower bound on $N(P_G)$ for Erdös-Renyi graphs. Furthermore, with high probability, G has a facet subgraph that supports exactly the facet hyperplanes supported by the same bipartition on the complete graph.

While the trends seen when we sample from $G(n,p)$ have no apparent connection to the average local clustering coefficient, which is p, correlations are observed when we consider different approaches to sampling graphs. An exhaustive computation for all connected graphs on eight vertices shows a positive correlation between average local clustering and number of facets. Using Markov Chain Monte Carlo methods to sample from the space of connected graphs with a fixed number of vertices and edges, we see that graphs with higher C_{WS} tend to produce polytopes with more facets. Additionally, data from these ensembles indicates that the variance in facet counts tends to increase as C_{WS} increases. When we further restrict to the space of connected graphs with fixed degree sequence (in particular graphs with hubs and k-regular graphs), this correlation remains and we observe less change in variance.

Chapter 4 Descriptions of Computational Experiments

In general, it is difficult to determine the number of facets of a polytope [27], particularly as dimension increases. The combinatorial description of facet-defining functions for symmetric edge polytopes given in [15, Theorem 3.1] is a useful theoretical starting point for counting facets. The work of Chen, Davis, and Korchevskaia [6] in describing facet subgraphs also offers a helpful starting point for computations. However, these descriptions do not offer any particular insight into how graph structure affects facet counts. Therefore, an aim of our experimentation was to generate ensembles of examples and look for patterns and relationships between graph structure and facet structure. Even with the aid of computational tools, in general, it is difficult and costly to determine the number of facets of a polytope [27], particularly as dimension increases. For this reason, we chose to narrow our focus to polytopes of dimension at most 19 arising from graphs with at most 20 vertices.

Throughout this work, data collected from computational experiments has been invaluable for generating examples as well as forming and supporting conjectures. All computations for these experiments were performed using SageMath [29], a language built on Python [30] that has some additional functionality for mathematics applications. For our purposes, SageMath is well-suited to generating graphs, sampling from graph spaces, and computing clustering metrics. For facet computations, we relied on Normaliz [4], an open source tool designed for the study of polyhedral geometry.

4.1   Complete Enumerations

Within SageMath, the package nauty [20] computes automorphism groups for graphs. Contained in nauty are generators for many classes of graphs up to isomorphism.

Throughout this work with symmetric edge polytopes, we used nauty to generate all non-isomorphic, connected graphs with a fixed number of vertices. Constructing the symmetric edge polytopes for these graphs and computing their facets with Normaliz gave significant evidence toward Conjectures 2.2.4 and 2.0.2 regarding the structures of graphs with extremal numbers of facets. Generating all connected graphs with a fixed number of vertices also allowed us to create plots like that in Figure 3.1, which motivated the investigation of average local clustering in relation to facet counts.

4.2   Sampling from Random Graph Models

Motivated by the correlation seen in our complete enumerations for small numbers of vertices, we explored ensembles of connected graphs generated by three different random graph models that each restricted the types of graphs we considered in different ways.

4.2.1 Erdös-Renyi Model ($G(n,p)$)

The Erdös-Renyi model is widely used and well-understood. It served as a good starting point as it gave hope for some theoretical results, and its implementation in SageMath already existed. As discussed in Section 3.1, a relationship between number of facets and average local clustering was not apparent in the samples taken from $G(n,p)$. Therefore we set aside some of the desire for theoretical results to employ other models that could restrict the space differently.

4.2.2 Sampling via Markov Chain Monte Carlo Techniques

The visualization of a Markov chain traversal as taking a random walk through a graph of graphs was discussed in Section 3.2. To implement this process in SageMath, we needed to determine a starting point for each ensemble as well as a frequency at which we would sample (i.e., how many steps would we take on the walk before "picking up" the next graph).

Our sampling method for $\mathcal{G}(n.m)$ began by generating a random element G from $G(n,p)$. Thus the number of edges m for the graphs in the sample was determined by the size of the edge set of G. We then successively randomly choose an edge $e \in E(G)$ and a non-edge $f \in E(G)^C$ to generate the next step in a random walk on the graph of graphs. We use subsampling, typically taking every 11-th graph, in an attempt to generate an ensemble of graphs with more diverse structures, though, due to computational constraints, our sample sizes are not particularly large. Note that the subsampling frequency was not chosen based on any information about the target distribution or mixing time.

Our sampling method for $\mathcal{G}(\mathbf{d}$ was similar. We began by generating a connected graph with degree sequence $\mathbf{d}$ via the Havel-Hakimi algorithm [13] and randomly performing double-edge swaps. Again, we employed subsampling, typically taking every 5-th or 11-th graph depending on the number of vertices. As before, our subsampling frequency was not based on any information regarding the target distribution or mixing time.

4.3 An Exploration of Connected $B(A,G)$

In service of counting or bounding the number of facets of symmetric edge polytopes, it would be useful to understand how many and which induced bipartite subgraphs are facet subgraphs for a given G, particularly in the case where G is connected and sparse. Toward this end, we can consider plots such as Figure 4.1, which shows the results of an experiment identifying facet subgraphs of some 11-regular graphs on 5000 vertices. To create this plot, we generated ten 11-regular connected graphs on 5000 vertices using double-edge swap MCMC, sampling after every 100001 swaps. For each graph G, a sequence of 5000 random subsets $(A_1, \ldots, A_{5000})$ of the vertex set V was generated. For each $0 < 10j \leq 5000$, we compute the fraction b_{10j} of the subsets in $(A_1, \ldots, A_{10j})$ which induce connected bipartite subgraphs $B(A_i, G)$ and plot the point $(10j, b_{10j})$. This process yields a sequence plot for each sampled graph. As can
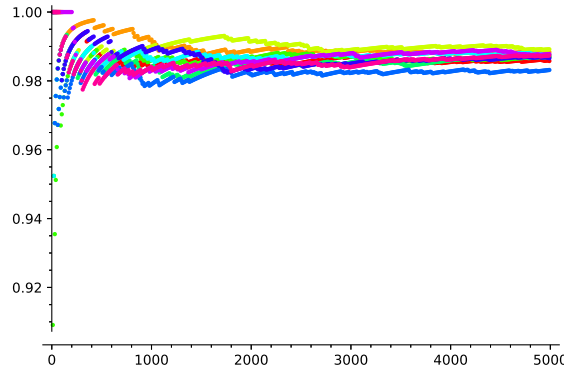
Figure 4.1: A collection of sequence plots for a sample of ten 11-regular connected graphs G on 5000 vertices showing how the fraction of sampled subsets A_i inducing a connected $B(A_i, G)$ changes over time and appears to stabilize near a value between 0.98 and 1.

be seen in this figure, as j increases, for each graph the fraction of subsets inducing a connected bipartite subgraph appears to stabilize near a value between 0.98 and 1. Note that this is an extremely small sample of the 2^{5000} subsets of the vertex set, and a small sample of 11-regular graphs. Nonetheless, these results are surprising given that these graphs, though large, are sparse with only $27,500$ of $12,497,500$ possible edges, or approximately 0.22%. An open question of interest is to determine, for a fixed k, asymptotic estimates for the expected number of induced bipartite subgraphs that are facet subgraphs for a k-regular graph on n vertices.

Bibliography

[1] M. Beck and S. Robins. *Computing the continuous discretely*. Undergraduate Texts in Mathematics. Springer, New York, second edition, 2015. Integer-point enumeration in polyhedra, With illustrations by David Austin.

[2] B. Braun and K. Bruegge. Facets of symmetric edge polytopes for graphs with few edges, 2022. preprint at https://arxiv.org/abs/2201.13303.

[3] B. Braun, K. Bruegge, and M. Kahle. Facets of random symmetric edge polytopes, degree sequences, and clustering, 2022.

[4] W. Bruns, C. S. B. Ichim, and U. von der Ohe. Normaliz. algorithms for rational cones and affine monoids. Available at https://normaliz.uos.de.

[5] W. Bruns, B. Ichim, and C. Söger. The power of pyramid decomposition in Normaliz. *J. Symbolic Comput.*, 74:513–536, 2016.

[6] T. Chen, R. Davis, and E. Korchevskaia. Facets and facet subgraphs of symmetric edge polytopes. *Discrete Applied Mathematics*, 328:139–153, 2023.

[7] T. Chen, R. Davis, and D. Mehta. Counting equilibria of the Kuramoto model using birationally invariant intersection index. *SIAM J. Appl. Algebra Geom.*, 2(4):489–507, 2018.

[8] T. Chen and E. Korchevskaia. Graph edge contraction and subdivisions for adjacency polytopes, 2020. preprint at https://arxiv.org/abs/1912.02841.

[9] A. D'Alì, E. Delucchi, and M. Michałek. Many faces of symmetric edge polytopes. *Electron. J. Comb.*, 29, 2019.

[10] A. D'Alì, M. Juhnke-Kubitzke, D. Köhne, and L. Venturello. On the gamma-vector of symmetric edge polytopes, 2022. https://arxiv.org/abs/2201.09835.

[11] R. J. Faudree and M. Simonovits. On a class of degenerate extremal graph problems. *Combinatorica*, 3(1):83–93, 1983.

[12] B. K. Fosdick, D. B. Larremore, J. Nishimura, and J. Ugander. Configuring random graph models with fixed degree sequences. *SIAM Review*, 60(2):315–355, 2018.

[13] S. L. Hakimi. On realizability of a set of integers as degrees of the vertices of a linear graph ii. uniqueness. *Journal of the Society for Industrial and Applied Mathematics*, 11(1):135–147, 1963.

[14] M. Henk, J. Richter-Gebert, and G. M. Ziegler. Basic properties of convex polytopes. In *Handbook of discrete and computational geometry*, CRC Press Ser. Discrete Math. Appl., pages 243–270. CRC, Boca Raton, FL, 1997.

[15] A. Higashitani, K. Jochemko, and M. Michałek. Arithmetic aspects of symmetric edge polytopes. *Mathematika*, 65(3):763–784, 2019.

[16] O. F. Inc. The On-Line Encyclopedia of Integer Sequences. Published electronically at https://oeis.org/A027383, Sequence A027383.

[17] O. F. Inc. The On-Line Encyclopedia of Integer Sequences, 2023. Published electronically at https://oeis.org.

[18] T. Kálmán and L. Tóthmérész. Ehrhart theory of symmetric edge polytopes via ribbon structures, 2022. https://arxiv.org/abs/2201.10501.

[19] T. Matsui, A. Higashitani, Y. Nagazawa, H. Ohsugi, and T. Hibi. Roots of ehrhart polynomials arising from graphs. *Journal of Algebraic Combinatorics*, 34(4):721–749, May 2011.

[20] B. D. McKay and A. Piperno. Practical graph isomorphism, ii. *Journal of Symbolic Computation*, 60:94–112, 2014.

[21] M. Newman. *Networks*. Oxford University Press, Oxford, 2018.

[22] B. Nill. Classification of pseudo-symmetric simplicial reflexive polytopes. In *Algebraic and geometric combinatorics*, volume 423 of *Contemp. Math.*, pages 269–282. Amer. Math. Soc., Providence, RI, 2006.

[23] H. Ohsugi and K. Shibata. Smooth Fano polytopes whose Ehrhart polynomial has a root with large real part. *Discrete Comput. Geom.*, 47(3):624–628, 2012.

[24] H. Ohsugi and A. Tsuchiya. The h^*-polynomials of locally anti-blocking lattice polytopes and their γ-positivity. *Discrete & Computational Geometry*, 66(2):701–722, Aug 2020.

[25] H. Ohsugi and A. Tsuchiya. Symmetric edge polytopes and matching generating polynomials. *Combinatorial Theory*, 1(0), Dec 2021.

[26] H. Robbins. A remark on Stirling's formula. *The American Mathematical Monthly*, 62(1):26–29, Jan 1955.

[27] R. Seidel. Convex hull computations. In *Handbook of discrete and computational geometry*, CRC Press Ser. Discrete Math. Appl., pages 361–375. CRC, Boca Raton, FL, 1997.

[28] R. P. Stanley. *Catalan numbers*. Cambridge university press, Cambridge, 2015.

[29] The Sage Developers. *SageMath, the Sage Mathematics Software System (Version 9.3)*, 2021. https://www.sagemath.org.

[30] G. Van Rossum and F. L. Drake Jr. *Python reference manual*. Centrum voor Wiskunde en Informatica Amsterdam, 1995.

[31] D. J. Watts and S. H. Strogatz. Collective dynamics of 'small-world' networks. *Nature*, 393(6684):440–442, 1998.

[32] G. M. Ziegler. *Lectures on polytopes*, volume 152 of *Graduate Texts in Mathematics*. Springer-Verlag, New York, 1995.

Kaitlin Elizabeth Bruegge

Education:

- University of Kentucky, Lexington, KY

    – Ph.D., Mathematics   *expected August 2023*
    – M.A., Mathematics   *December 2020*

- Xavier University, Cincinnati, OH

    – B.S., Summa cum Laude, Mathematics   *May 2018*
    – B.A., Summa cum Laude, Computer Science   *May 2018*

Professional Positions:

- Assistant Professor Educator, University of Cincinnati Fall 2023–

- Graduate Teaching Assistant, University of Kentucky Fall 2018–Spring 2023

Honors

- College of Arts and Sciences Certificate for Outstanding Teaching, University of Kentucky

- Department of Mathematics Diversity, Equity, and Inclusion Award, University of Kentucky

- Carl Lee Excellence in Teaching Award, University of Kentucky

- Max Steckler Fellowship, University of Kentucky

Publications & Preprints:

- "Facets of Symmetric Edge Polytopes for Graphs with Few Edges," with Benjamin Braun, arXiv:2201.13303 (submitted).

- "Triangulations of Flow Polytopes, Ample Framings, and Gentle Algebras", with Matias von Bell, Benjamin Braun, Derek Hanely, Zachery Peterson, Khrystyna Serhiyenko, and Martha Yip, arXiv:2203.01896 (submitted).

- "Facets of Random Symmetric Edge Polytopes, Degree Sequences, and Clustering", with Benjamin Braun and Matthew Kahle, arXiv:2204.07239 (submitted).

- "Alexander Duals of Symmetric Simplicial Complexes and Stanley-Reisner Ideals," with Ayah Almousa, Martina Juhnke-Kubitzke, Uwe Nagel, and Sasha Pevzner, arXiv:2209.14132 (submitted).